



TDOT
Department of
Transportation



Investigating the Long-term Frictional Properties and Establishing Aggregate Polishness Guidelines for Asphalt Surface Mixtures in Tennessee

Research Final Report from University of Tennessee, Knoxville | Baoshan Huang, Jingtao Zhong, Kai Huang, Yuetan Ma, Pawel Polaczyk | April 30, 2025

Sponsored by Tennessee Department of Transportation Strategic Planning, Research & Innovation Division

Research Office & Federal Highway Administration



DISCLAIMER

This research was funded through the State Planning and Research (SPR) Program by the Tennessee Department of Transportation and the Federal Highway Administration under **RES 2023-15: Research Project Title: Investigating the Long-term Frictional Properties and Establishing Aggregate Polishness Guidelines for Asphalt Surface Mixtures in Tennessee.**

This document is disseminated under the sponsorship of the Tennessee Department of Transportation and the United States Department of Transportation in the interest of information exchange. The State of Tennessee and the United States Government assume no liability of its contents or use thereof.

The contents of this report reflect the views of the author(s) who are solely responsible for the facts and accuracy of the material presented. The contents do not necessarily reflect the official views of the Tennessee Department of Transportation or the United States Department of Transportation.

Technical Report Documentation Page

1. Report No. RES2023-15	2. Government Accession No.	3. Recipient's Catalog No.	
4. Title and Subtitle <i>Investigating the Long-term Frictional Properties and Establishing Aggregate Polishness Guidelines for Asphalt Surface Mixtures in Tennessee</i>		5. Report Date April 2025	
		6. Performing Organization Code	
7. Author(s) Baoshan Huang, Jingtao Zhong, Kai Huang, Yuetan Ma, Pawel Polaczyk		8. Performing Organization Report No.	
9. Performing Organization Name and Address Department of Civil and Environmental Engineering The University of Tennessee, Knoxville 851 Neyland Drive Knoxville, TN, 37996		10. Work Unit No. (TRAVIS)	
		11. Contract or Grant No. RES2023-15	
12. Sponsoring Agency Name and Address Tennessee Department of Transportation 505 Deaderick Street, Suite 900 Nashville, TN 37243		13. Type of Report and Period Covered	
		14. Sponsoring Agency Code	
15. Supplementary Notes Conducted in cooperation with the U.S. Department of Transportation, Federal Highway Administration.			
16. Abstract The frictional properties of aggregates play a significant role in determining pavement skid resistance. To preserve natural aggregates, reclaimed asphalt pavement (RAP) has been widely used for decades. However, its application in pavement surface courses is restricted due to uncertainties about its frictional properties and other mechanical performance. Therefore, this research aimed to quantitatively assess both aggregates and RAP to develop a quick evaluation method for frictional properties. Additionally, long-term frictional properties of asphalt mixtures commonly used in Tennessee were investigated to establish correlation with different testing devices. Three-wheel polishing device (TWPD) was employed to simulate the long-term traffic polishing in laboratory. Dynamic friction tester (DFT) and Circular track meter (CTM) were utilized for both laboratory and field skid resistance measurement tests. The locked-wheel skid trailer (LWST) was also employed to compare results with those from the DFT. DFT proves to be a practical tool for friction assessment with both laboratory and field applications, which can be used for the development of friction performance-based mixture designs. Results indicate a significant correlation between SiO ₂ content and frictional properties of aggregates. Furthermore, the relationship is identified between the percentage of polish-resistant aggregates and the decrease in the coefficient of friction (COF) in asphalt mixtures.			
17. Key Words AGGREGATE, RAP, ASPHALT MIXTURE, PAVEMENT SKID RESISTANCE, FRICTION, TEXTURE		18. Distribution Statement No restriction. This document is available to the public from the sponsoring agency at the website http://www.tn.gov/ .	
19. Security Classif. (of this report) Unclassified	20. Security Classif. (of this page) Unclassified	21. No. of Pages	22. Price

Acknowledgement

We would like to begin by thanking the Tennessee Department of Transportation (TDOT) for funding this research project. We have continued to collaborate closely with regional engineers and local technicians at the TDOT Materials and Test Division and local asphalt plants. They have provided valuable support towards the fulfillment of the research objectives. Without their support, it would be impossible for us to finish this research project. We would also like to thank the administrative staff from the TDOT Research Office who have worked very closely with our research team and kept the whole project on the proposed schedule. We also would like to show our gratitude to the federal highway administration (FHWA) for supporting the skid resistance tests of surface materials.

Executive Summary

Highway traffic accidents often occur due to inadequate pavement skid resistance, particularly on rainy days when water-related friction loss becomes a significant concern. Ensuring adequate pavement friction can enhance driving safety, ultimately reducing the frequency of traffic accidents. Therefore, it is important to provide adequate pavement skid resistance.

The purpose of this study was to investigate the frictional properties of aggregates, reclaimed asphalt pavement (RAP), and asphalt mixtures in Tennessee to provide sufficient skid resistance. To conserve natural aggregates, RAP has been widely used for decades. However, its application in pavement surface courses is often restricted due to uncertainties about its frictional properties and other mechanical performance. Additionally, the current mix design specification does not use a performance related test for skid resistance of asphalt mixtures.

Therefore, this research aimed at enhancing the pavement skid resistance at both aggregate and asphalt mixture perspectives. This research attempted to quantify the micro-texture frictional properties of aggregates determined by polishing and abrasion tests. X-ray fluorescence (XRF) analysis was employed to accurately quantify the silica dioxide (SiO_2) content in various aggregate samples, establishing correlations with polished stone value (PSV), Micro-Deval (MD) abrasion loss, and surface morphological characteristics, as assessed through the aggregate image measurement system (AIMS). This approach aimed to provide a rapid and efficient method for measuring SiO_2 content in reclaimed asphalt pavement (RAP), comparing values from laboratory-produced RAP with those from field-sampled RAP to ensure consistency and reliability.

The surface skid resistance of laboratory asphalt mixtures as well as field pavements has been investigated. To assess skid resistance comprehensively, both the Dynamic Friction Tester (DFT) and the Circular Track Meter (CTM) were used for skid resistance tests in both laboratory and field conditions. Three-wheel polishing device (TWPD) was employed to simulate the long-term traffic polishing in laboratory to observe the deterioration of coefficient of friction (COF) and texture.

Additionally, the locked-wheel skid trailer (LWST) was used to validate and compare the results obtained from the DFT, providing a robust evaluation of frictional properties. Field pavement skid resistance tests were conducted in a total of 11 segments in Tennessee, covering the most commonly used aggregates. Field cores were collected and analyzed by XRF to investigate the impact of chemical composition on pavement skid resistance.

This approach attempted to enhance the understanding of skid resistance and support the development of specifications for reliable surface course materials that meet friction and durability requirements.

Key Findings

- There is no significant difference between the slab and ring-shaped specimens for COF and texture parameters, measured by DFT and CTM. The ring-shaped specimen could be used as an alternative method to evaluate the skid resistance in the laboratory.
- The uniformity of aggregates plays a critical role in accurately measuring SiO_2 content via XRF. It is recommended to use aggregates passing 3/8 in. (9.5mm) and retained on No.4 (4.75mm) sieves for SiO_2 content measurement for both aggregates and RAP, ensuring a

more reliable test result. The SiO₂ of RAP treated either by Trichloroethylene (TCE) or hammer can be efficiently measured by XRF.

- Correlation between the SiO₂ content and frictional properties of aggregates and RAP has been established. SiO₂ content has shown significant correlations with PSV, and texture loss, with R² Values of 0.81, and 0.78 respectively. With the increase of SiO₂ contents, PSV also increases while relative texture loss decreases.
- DFT measures friction on a circular path, which captures both polished and unpolished areas of the pavement in the field, potentially leading to higher average values. LWST measures friction directly on the wheel path, resulting in lower average values compared to COF.
- The COF values for the left and right wheel paths are generally comparable across all segments, with no significant differences observed. In most segments, the COF values for the left and right wheel paths are within close range, indicating similar frictional properties across both paths.
- The multiple linear regression model, which incorporates both silica-iron mineral content and polish-resistant aggregate percentage, explaining 88% of the variation in terminal COF. The result indicates that the model provides a reliable representation to determine the terminal COF.

Key Recommendations

- It is recommended that the DFT integrated with laboratory accelerated polishing tests supports the development of friction performance-based mixture designs.
- It is recommended to use aggregates passing 3/8 in. (9.5mm) and retained on No.4 (4.75mm) sieves for SiO₂ content measurement for both aggregates and RAP, ensuring a more reliable test result.
- It is suggested that considering the combination of silica and iron content (SiO₂+Fe₂O₃) in the analysis provides a better prediction of changes in COF. Asphalt mixture with slag shows a significantly lower decrease in COF, supporting the role of slag in improving skid resistance due to its rich iron content.
- According to the regression analysis, if the polish-resistant aggregate content remains at 75%, a minimum of 50% overall silica-iron content is required to achieve a terminal COF (measured by DFT) greater than 0.35 based on laboratory findings.
- At a constant level of polish-resistant aggregate percentage, increasing the silica-iron mineral content leads to a higher terminal COF, thereby enhancing pavement skid resistance.

Table of Contents

DISCLAIMER.....	i
Technical Report Documentation Page.....	ii
Acknowledgement.....	iii
Executive Summary	iv
Key Findings.....	iv
Key Recommendations.....	v
List of Tables.....	viii
List of Figures	ix
Glossary of Key Terms and Acronyms	xi
Chapter 1 Introduction	1
1.1 Problem Description	1
1.2 Objectives of the Research	1
1.3 Scope of Work.....	1
Chapter 2 Literature Review	3
2.1 Introduction.....	3
2.2 Friction mechanism	3
2.3 Pavement skid resistance design and evaluation	4
2.3.1 Materials selection.....	4
2.3.2 Silica content detection method.....	5
2.4 Pavement skid resistance evaluation methods.....	5
2.4.1 Friction coefficient-based measurement methods	5
2.4.2 Texture-based methods	7
2.5 Research gaps.....	8
Chapter 3 Methodology.....	9
3.1 Measurement of chemical composition in aggregates.....	9
3.2 Micro-Deval test for abrasion evaluation	9
3.3 Micro-texture measured by Aggregate Image Measurement System	10
3.4 Materials	11
3.4.1 Aggregates type and source.....	11
3.4.2 Reclaimed asphalt pavement.....	12
3.4.3 Asphalt mixtures collection	14
3.4.4 Sample fabrication	14

3.5 Frictional performance tests.....	15
3.5.1 Polishing device.....	16
3.5.2 Dynamic friction tester	17
3.5.3 Circular Track Meter.....	18
3.6 Field pavement skid resistance test.....	20
3.6.1 Selection of test segments.....	20
3.6.2 Skid resistance test setup.....	20
3.6.3 Locked wheel skid trailer from TDOT.....	22
Chapter 4 Results and Discussion	24
4.1 Analysis for aggregate skid resistance	24
4.1.1 Correlation between SiO ₂ and PSV.....	24
4.1.2 Correlation between SiO ₂ and Micro-Deval test.....	27
4.1.3 Correlation between SiO ₂ and AIMS test.....	27
4.1.4 SiO ₂ content of RAP.....	30
4.2 Analysis of laboratory asphalt mixtures.....	32
4.2.1 Comparison between slab-based and ring-shaped specimens.....	32
4.2.2 Deterioration analysis of laboratory asphalt mixture skid resistance.....	39
4.3 Field skid resistance measurement	42
Chapter 5 Conclusion	49
References	51
Appendices	53

List of Tables

Table 2-1 Pavement friction measurement.....	5
Table 2-2 Pavement texture measurement.	7
Table 3-1 Aggregate type and source.....	11
Table 3-2 Collected plant mixtures used for laboratory tests.	14
Table 3-3 Polishing revolution (cycles).	16
Table 4-1 AIMS results.	28
Table 4-2 Test results of crushed laboratory-produced RAP.....	31
Table 4-3 SiO ₂ contents of field-sampled RAP.	32
Table 4-4 Results of slab-based asphalt mixture specimen.	32
Table 4-5 Results of ring-shaped asphalt mixture specimen.....	35
Table 4-6 Frictional-based performance results.....	39
Table 4-7 Terminal COF Prediction performance of regression models.....	42
Table 4-8 Summary of the field test segments.....	46

List of Figures

Figure 2-1 Tire-pavement interaction [4].	3
Figure 2-2 Mechanism of pavement-tire interaction [9].	4
Figure 2-3 Dynamic friction tester.	6
Figure 2-4 Friction-based pavement skid resistance testing devices [2].	7
Figure 2-5 Texture-based pavement skid resistance testing devices [2].	8
Figure 3-1 Portable benchtop XRF.	9
Figure 3-2 Micro-Deval test.	10
Figure 3-3 AIMS device and analysis software.	10
Figure 3-4 Aggregate coupons for frictional test.	12
Figure 3-5 Polishing and testing of prepared aggregate coupons.	12
Figure 3-6 Processed RAP by hammer and TCE.	13
Figure 3-7 Laboratory preparation of RAP.	13
Figure 3-8 Heated asphalt roller compactor.	15
Figure 3-9 Design schematic of test ring.	15
Figure 3-10 Fabrication of ring-shaped and slab-based specimens.	15
Figure 3-11 Three-wheel polishing device.	16
Figure 3-12 Prepared specimens for polishing.	17
Figure 3-13 Indoor DFT test.	18
Figure 3-14 Structure sketch of DFT.	18
Figure 3-15 World Road Association (PIARC) texture definitions and their influence on pavement surface characteristics [26].	19
Figure 3-16 Indoor pavement texture test via CTM.	20
Figure 3-17 2D Profile obtained from CTM.	20
Figure 3-18 Schematic for the field pavement skid resistance test.	21
Figure 3-19 Field pavement skid resistance performance test.	21
Figure 3-20 Locked wheel skid trailer from TDOT.	22
Figure 3-21 Tire configuration of the LWST.	23
Figure 4-1 Polishing-resistant performance comparison before and after polishing.	24
Figure 4-2 Chemical composition in limestones: (a) SiO ₂ content in limestone; and (b) CaO content in limestone.	25
Figure 4-3 Correlation between PSV and chemical composition: (a) correlation between SiO ₂ and PSV; and (b) correlation between CaO and PSV.	26
Figure 4-4 MD abrasion loss results: (a) correlation between MD loss and PSV; and (b) correlation between MD loss and SiO ₂ .	27
Figure 4-5 Image-based evaluation metrics.	29
Figure 4-6 Angularity and texture change with different SiO ₂ contents: (a) correlation between angularity loss and SiO ₂ ; and (b) correlation between texture loss and SiO ₂ .	29
Figure 4-7 SiO ₂ of laboratory-produced RAP with different treatments.	30
Figure 4-8 DFT results of five replicate tests during different polishing cycles based on slab specimens.	35
Figure 4-9 DFT changes on slab with incremental polishing cycles.	35
Figure 4-10 DFT changes with incremental polishing cycles based on ring specimens.	38
Figure 4-11 Correlation between decrease of COF ₁ and chemical composition.	40
Figure 4-12 Correlation between decrease of COF ₂ and chemical composition.	40
Figure 4-13 Correlation between decrease of COF and polish-resistant percentage.	41
Figure 4-14 Correlation between terminal COF and polish-resistant materials.	41
Figure 4-15 DFT and IFI from collected data.	43
Figure 4-16 (a) Correlation between IFI and DFT60; (b) Correlation between IFI and DFT20.	43
Figure 4-17 Correlation between MPD and COF at 60km/h (DFT60).	44
Figure 4-18 Correlation between MPD and MTD.	44
Figure 4-19 Field friction measurements by DFT and LWST.	45

Figure 4-20 COF measured by DFT on different wheel paths.....	45
Figure 4-21 Collected field cores for the analysis of chemical composition.....	47
Figure 4-22 Silica content distribution over 11 segments.....	47
Figure 4-23 Decrease in COF compared with service year, AADT, and silica content.	48

Glossary of Key Terms and Acronyms

RAP: Reclaimed Asphalt Pavement

XRF: X-ray Fluorescence

TCE: Trichloroethylene

BPT: British Pendulum Tester

BPN: British Pendulum Number

PSV: Polished Stone Value

DFT: Dynamic Friction Tester

CTM: Circular Track Meter

TWPD: Three-wheel Polishing Device

SPT: Sand Patch Test

COF: Coefficient of Friction

AIMS: Aggregate Image Measurement System

FHWA: Federal Highway Administration

NCAT: National Center for Asphalt Technology

PIARC: Permanent International Association of Road Congress

IFI: International Friction Index

SN/FN: Skid/Friction Number

ASTM: American Society for Testing and Materials

LWST: Locked-wheel Skid Trailer

Chapter 1 Introduction

1.1 Problem Description

The skid resistance of asphalt mixtures is characterized by micro- and macro-textures. The micro-texture is associated with the polishing properties of aggregates at the mixture surface. The macro-texture is related to gradation, density, shape, angularity, and arrangement of aggregates within the mixture layer. TDOT controls the micro-texture of surface asphalt mixtures by requiring a minimum of 75% of polish-resistant aggregates. However, this requirement is based on limited field experimentation conducted by TDOT engineers many years ago. In addition, the routine use of reclaimed asphalt pavement (RAP) poses new challenges due to the unknown amount of siliceous materials in the RAP materials. The asphalt mixture design has not considered the friction performance-based tests, and no quantitative methods are used to guarantee the deterioration of pavement skid resistance.

Additionally, some regions of Tennessee experience high costs for importing polish-resistant aggregates for asphalt surface mixtures. The lack of locally available polish-resistant aggregate sources can require contractors to transport polish-resistant aggregates at a great expense. Aggregates are a non-renewable resource that should be used with sustainability. Therefore, it is imperative to quantify the required friction levels of surface mixtures in Tennessee.

1.2 Objectives of the Research

The objectives of the proposed study are to:

- Correlate the long-term frictional properties of asphalt mixtures commonly used in Tennessee with a practical engineering performance tester, such as the dynamic frictional tester (DFT).
- Compare the frictional properties using the DFT with the current friction testing methods used in TN, such as the Locked Wheel Trailer, etc.
- Examine the validity of the 75% minimum polish-resistant materials required for the surface asphalt mixtures in Tennessee.
- Develop a practical method to determine the siliceous aggregate content in RAP quickly.
- Recommend specification limits for blending aggregates as well as performance-based testing limits that provide adequate frictional properties.

1.3 Scope of Work

The scope of the research work includes:

- To complete synthesis of a literature review on pavement friction and to conduct a DOT survey on measures in their specifications and mix design requirements to provide insights for improved pavement design and material selection.
- To evaluate the micro-textural frictional properties of Tennessean aggregates.
- To identify or develop aggregate tests for evaluating the silica content in aggregates.
- To evaluate and optimize the macro-textural frictional properties of Tennessean surface asphalt mixtures.

- To conduct a statistical analysis on the test results and correlate the fundamental properties of asphalt mixture and aggregate to frictional properties.
- To make recommendations to TDOT specifications regarding materials selection.

Chapter 2 Literature Review

2.1 Introduction

The direct force developed by tire-pavement interaction is skid resistance, which is useful for braking on pavements [1]. Many highway traffic accidents happen due to inadequate pavement skid resistance, especially on rainy days, and car accidents happen more frequently due to water-oriented pavement friction decay. Adequate pavement skid resistance is essential for ensuring driving safety and comfort, helping to reduce the risk of traffic accidents. Therefore, pavement skid resistance should be carefully designed and routinely evaluated [2].

Several factors influence asphalt pavement skid resistance, including pavement texture, weather conditions, and construction practices. Skid resistance results from the interaction between the tire and pavement, which is further affected by environmental conditions. It can be directly measured using the pavement friction coefficient and indirectly evaluated through pavement texture indices [2]. Pavement texture is the primary factor influencing pavement friction and can be categorized into four levels defined by the wavelength: unevenness/roughness (>500mm), mega-texture (50-500mm), macro-texture (0.5-50mm), and micro-texture (<0.5mm). Among these, macro-texture and micro-texture are the most critical in determining pavement friction performance, as illustrated in Figure 2-1 [3].

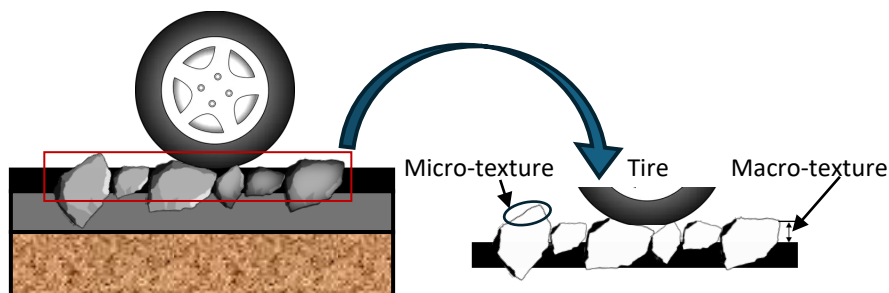


Figure 2-1 Tire-pavement interaction [4].

Micro-texture refers to the small-scale texture of aggregate surfaces and plays a crucial role in providing skid resistance at low speeds. Its long-term consistency primarily depends on the properties of the aggregates, particularly their resistance to abrasion and polishing. Macro-texture, on the other hand, is mainly influenced by asphalt mixture gradation and mix design. It results from the uneven distribution of the mixture and is especially important for maintaining skid resistance at high speeds and under wet conditions. Both macro-texture and micro-texture are critical to pavement skid resistance performance. Therefore, a thorough investigation of pavement textures is essential to enhance driving safety and ensure better road performance for users [5-7].

2.2 Friction mechanism

Pavement friction results from the complex interaction of two primary frictional force components—adhesion and hysteresis, as shown in Figure 2-2. Adhesion, which occurs at the pavement-tire interface, is primarily influenced by the micro-texture of the aggregate, providing

surface contact, particularly at low speeds and under dry conditions. This component is significantly affected by aggregate mineralogy and surface roughness [8, 9]. In contrast, hysteresis is generated within the tire due to deformation caused by macro-texture, leading to energy dissipation as the tire deforms and recovers while rolling over surface irregularities. Macro-texture plays a dominant role in high-speed and wet conditions, where water drainage from the contact area is essential to prevent hydroplaning. The depth and distribution of macro-texture are influenced by the aggregate gradation, mix design, and compaction process [8, 9].

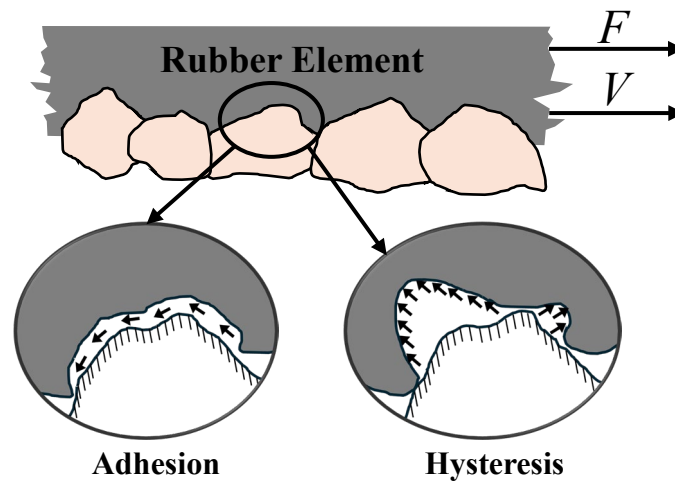


Figure 2-2 Mechanism of pavement-tire interaction [9].

2.3 Pavement skid resistance design and evaluation

Selecting suitable materials for asphalt mixtures is crucial to ensuring adequate skid resistance for pavements. The choice of appropriate aggregate types, asphalt binders, and mixture designs plays a vital role in developing sufficient skid resistance to enhance driving safety [10]. In addition to material selection, regular monitoring and maintenance of pavement skid resistance are essential for evaluating pavement conditions and implementing effective management strategies. Routine assessments help identify potential issues early and allow for timely corrective measures to maintain optimal friction levels. Furthermore, the availability of simple and accurate skid resistance measurement methods is critical for transportation agencies to efficiently monitor pavement performance and ensure road safety [2].

2.3.1 Materials selection

Aggregate, asphalt binder, and asphalt mixture must meet pavement design requirements to ensure adequate skid resistance performance. For aggregates, resistance to wear, polishing, and abrasion is essential. Several tests are used to evaluate aggregate properties, including the Los Angeles (LA) abrasion test, Polished Stone Value (PSV) test, and the Micro-Deval test. Limestone is a commonly used aggregate in pavement construction while it is susceptible to polishing. To enhance the pavement's resistance to polishing and ensure adequate skid performance, siliceous aggregates are blended with limestone. Monitoring the silica content in these mixtures is crucial for maintaining long-term skid resistance.

Regarding asphalt mixtures, proper aggregate arrangement is critical to achieving an interlocked structure that enhances pavement friction. Gradation types such as open-graded and gap-graded mixtures are effective in improving skid resistance. Pavement surfaces designed with Stone Mastic Asphalt (SMA) and Open-Graded Friction Courses (OGFC) offer optimized skid resistance by enhancing surface texture and drainage capabilities.

2.3.2 Silica content detection method

When used in hot-mix asphalt (HMA) pavements, aggregates composed of pure limestone tend to become polished as the pavement wears over time. To enhance resistance to wear and improve skid resistance, siliceous aggregates are blended with limestone. The standard test method for determining silica content in aggregates is outlined in “ASTM C25-17: Standard Test Methods for Chemical Analysis of Limestone, Quicklime, and Hydrated Lime” [11]. However, this standard method is complex and time-consuming for routine testing. The test includes three procedures and applies acids like hydrochloric, hydrofluoric, and sulfuric. All these acids are hazardous to use and pose a significant waste-disposal problem. Advanced techniques such as X-ray fluorescence (XRF) and Scanning Electron Microscopy (SEM) offer efficient alternatives for silica content detection. With these rapid detection methods, pavement skid resistance can be effectively evaluated and monitored.

2.4 Pavement skid resistance evaluation methods

Pavement skid resistance can be evaluated using two primary approaches: friction coefficient-based methods and texture-based methods. Friction coefficient-based methods directly measure the interaction between the tire and pavement surface under various conditions, providing a quantitative assessment of skid resistance. In contrast, texture-based methods indirectly evaluate skid resistance by analyzing the surface texture properties, such as macro-texture and micro-texture, which influence pavement friction performance.

2.4.1 Friction coefficient-based measurement methods

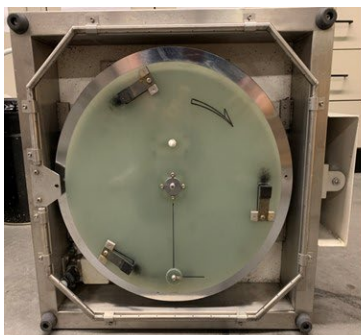
Friction coefficient-based measurements are direct methods to evaluate pavement skid performance. There are several devices to evaluate pavement friction level at a fixed or variable slip rate listed in Table 2-1.

Table 2-1 Pavement friction measurement.

<i>Test method</i>	<i>Representative equipment</i>	<i>Indices</i>
<i>Standard Test Method for Measuring Surface Frictional Properties Using the British Pendulum Tester [12]</i>	BPT (British Pendulum Test)	BPN
<i>Standard Test Method for Measuring Surface Frictional Properties Using the Dynamic Friction Tester [13]</i>	DFT (Dynamic friction tester)	Friction coefficient at different speed

<i>Standard Test Method for Skid Resistance of Paved Surfaces Using a Full-Scale Tire [14]</i>	Locked wheel skid trailer (LWST)	Friction number (FN) or Skid number (SN)
<i>Standard Test Method for Testing Side Force Friction on Paved Surfaces Using the Mu-Meter [15]</i>	SCRIM (Single test wheel with slip angle of 20 degrees)	SFC (sideway force coefficient)
	Mu-Meter (Double test wheels with each slip angle of 7.5 degrees)	
<i>Standard Test Method for Friction Coefficient Measurements Between Tire and Pavement Using a Variable Slip Technique [16]</i>	French IMAG	Friction number (FN)

Commonly used pavement friction measurement equipment is illustrated in Figure 2-3 and Figure 2-4. The Dynamic Friction Tester (DFT) is capable of measuring speed-dependent friction properties in both field and laboratory settings. For laboratory testing, specimens are prepared in slab or ring shapes, as shown in Figure 2-3. However, it is important to note that the DFT and the BPT provide friction measurements at a single spot on the pavement surface. In contrast, other methods depicted in Figure 2-4 are capable of achieving continuous friction measurements.



DFT



Field test



Lab test

Figure 2-3 Dynamic friction tester.



Figure 2-4 Friction-based pavement skid resistance testing devices [2].

2.4.2 Texture-based methods

Frequently used pavement texture measurement methods and equipment are shown in Table 2-2 and Figure 2-5. Pavement texture measurement can be categorized as volumetric techniques, water drainage rate techniques, and non-contact techniques. Non-contact techniques consist of laser scanning and image processing shown in Figure 2-5.

Table 2-2 Pavement texture measurement.

Test methods	Indices
Standard Test Method for Measuring Pavement Macrotexture Depth Using a Volumetric Technique [17]	MTD (Mean texture depth)
Standard Test Method for Measuring Pavement Texture Drainage Using an Outflow Meter [18]	MPD (Mean profile depth)
Standard Test Method for Measuring Pavement Macrotexture Properties Using the Circular Track Meter [19]	

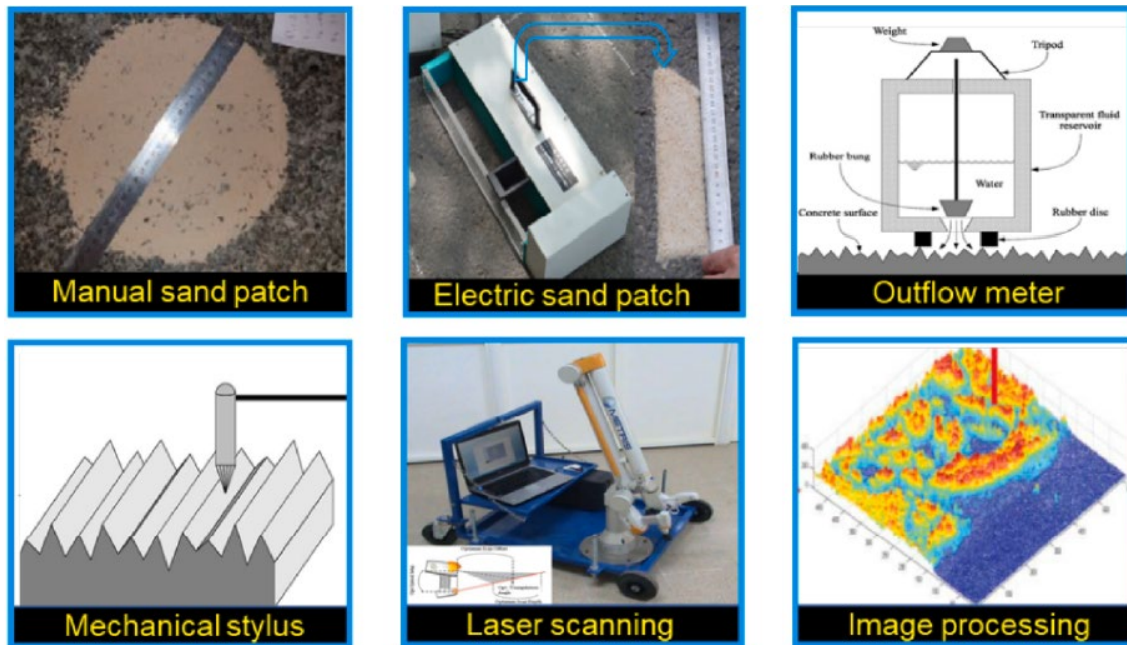


Figure 2-5 Texture-based pavement skid resistance testing devices [2].

2.5 Research gaps

As summarized from the literature reviews, there exist limited studies on the following areas:

1. No quantitative analysis for aggregate and RAP selection based on silica content.
2. The skid resistance-based performance tests have not been considered into mix design.
3. Inconsistent correlation between different devices for friction measurement.
4. Inadequate relationship modeling between friction and texture.

Chapter 3 Methodology

3.1 Measurement of chemical composition in aggregates

The non-destructive benchtop XRF was chosen to analyze the chemical composition of aggregates. As shown in Figure 3-1, a benchtop XRF is an integrated device with a built-in computer to provide fast and accurate test results. The X-ray emitter and receiver are embedded into this portable device, which takes three and a half minutes to analyze each sample. Samples were put into a container and X-ray was emitted to the specimen. XRF tested the exposed aggregate surface to analyze the chemical composition, and the uniformity of aggregates influenced the test results. Therefore, aggregates were screened into different sizes, and the average of three measurements was used to calculate the chemical composition. A total of four sizes of aggregates were tested, which were: (1) passing 5/8 in. (16mm) sieve, retained on 1/2 in. (12.5mm) sieve; (2) passing 1/2 in. (12.5mm) sieve, retained on 3/8 in. (9.5mm) sieve; (3) passing 3/8 in. (9.5mm) sieve, retained on No.4 (4.75mm) sieve; (4) passing No.4 (4.75mm) sieve, retained on No.8 (2.36mm) sieve.



Figure 3-1 Portable benchtop XRF.

3.2 Micro-Deval test for abrasion evaluation

The Micro-Deval (MD) test is used to measure the abrasion resistance of aggregates. MD test consists of a container with aggregates, steel balls and water to be rotated for abrasion. MD tests can be either controlled by revolution counts or running time. Aggregates went through the MD abrasion for 120 minutes in our experiment. As shown in Figure 3-2, after abrasion, the aggregates were screened using a 1.18 mm (No.16) sieve, and particles smaller than 1.18 mm were discarded when calculating the MD abrasion loss. Aggregates subjected to abrasion in the Micro-Deval (MD) test were subsequently used for Aggregate Image Measurement System (AIMS) analysis.



Figure 3-2 Micro-Deval test.

3.3 Micro-texture measured by Aggregate Image Measurement System

Aggregate shape characteristics, including texture, angularity, and form, are important micro-texture for pavement skid resistance. Rough aggregates offer greater skid resistance compared to smooth aggregates, while angular aggregates exhibit higher frictional properties than rounded ones. Aggregate Image Measurement System (AIMS) is used to quantify the surface characteristics of aggregates. As shown in Figure 3-3, this system was equipped with a digital camera and lighting units to capture the aggregate images, which were analyzed by wavelet analysis and gradient theory to calculate the angularity index and texture index [20].

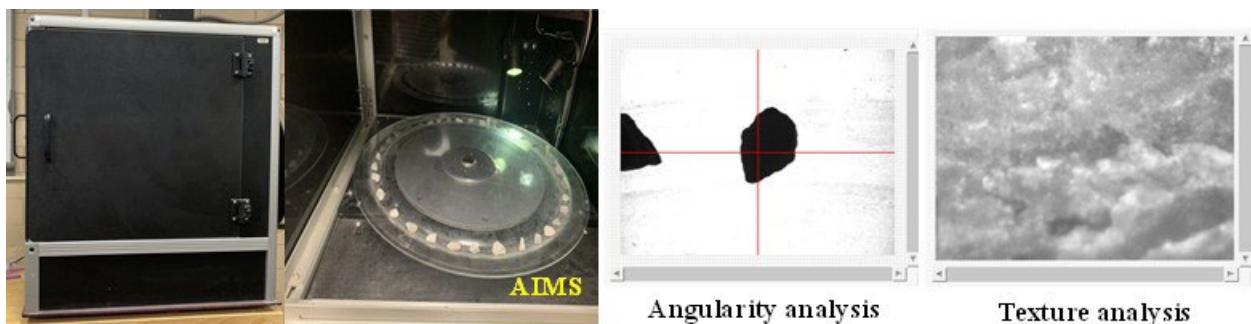


Figure 3-3 AIMS device and analysis software.

AIMS tests were conducted at the Turner-Fairbank Highway Research Center Geotechnical Laboratory of Federal Highway Administration (FHWA). Angularity is assessed using binary images of the aggregates, and for improved accuracy, the aggregates should be placed along the centerline of the rotation plate during testing. Aggregates were polished in the MD device for 120 minutes with 12,000 revolutions. AIMS testing was performed on the aggregates both before and after MD abrasion to evaluate abrasion loss and assess their relative resistance properties.

3.4 Materials

3.4.1 Aggregates type and source

Table 3-1 Aggregate type and source.

<i>Region</i>	<i>Material and source</i>
<i>Region 1</i>	Granite
	Gravel
	Slag
<i>Region 2</i>	Granite
	Slag
<i>Region 3</i>	Limestone#1
	Limestone#2
	Gravel#1
	Limestone#3
	Gravel#2
	Limestone#4
<i>Region 4</i>	Slag
	Gravel

A total of 13 local aggregates from Region 1, Region 2, Region 3, and Region 4 in Tennessee, commonly used for pavement surface layers, were selected for frictional characterization, as shown in Table 3-1. To effectively assess the polishing resistance of these aggregates, aggregate coupons (aggregates embedded in epoxy resin) were tested with BPT to evaluate their skid resistance levels. Aggregates were glued with epoxy resin and hardener to fabricate the curved aggregate coupons for the frictional test [21]. As illustrated in Figure 3-4, five curved specimens of each aggregate type were prepared for the polished stone value (PSV) test. The sand was applied to prevent epoxy resin from penetrating the specimen surface and affecting the test results. Aggregate coupons were subjected to an accelerated polishing machine after 9 hours at the National Center for Asphalt Technology (NCAT), as shown in Figure 3-5.



Figure 3-4 Aggregate coupons for frictional test.



Figure 3-5 Polishing and testing of prepared aggregate coupons.

3.4.2 Reclaimed asphalt pavement

Field-sampled reclaimed asphalt pavement (RAP) was generated by a cold-planing machine in Region 2 at State Route 50, Coffee County, Tennessee. To eliminate the influence of asphalt binder and expose the surface of original aggregates, milled RAP was processed using both mechanical and chemical methods, as shown in Figure 3-6.

The first method involves a straightforward mechanical approach—crushing the RAP with a hammer to break the material and expose a clean aggregate surface. The second method utilizes a Trichloroethylene (TCE) solution, which is applied through multiple extraction operations to dissolve and remove the asphalt binder effectively. Both methods are employed to ensure that the aggregates are free from residual asphalt, allowing for accurate analysis and evaluation of their properties.



Figure 3-6 Processed RAP by hammer and TCE.

To evaluate the effectiveness of the processing methods for RAP, the laboratory-produced artificial RAP was prepared to validate the measurement approach, ensuring the actual SiO_2 content was known before being coated with asphalt. Firstly, the original SiO_2 content of virgin aggregates was measured prior to asphalt coating. Secondly, Virgin aggregates were mixed with asphalt binder in the laboratory and subjected to oven aging to simulate long-term field aging. In this study, the laboratory-produced RAP was fabricated with different aggregate sizes to simplify the measurement process. The aggregate sizes used were: (1) passing 5/8 in. (16mm) sieve, retained on 1/2 in. (12.5mm) sieve; (2) passing 1/2 in. (12.5mm) sieve, retained on 3/8 in. (9.5mm) sieve; (3) passing 3/8 in. (9.5mm) sieve, retained on No.4 (4.75mm) sieve. Limestone aggregates are susceptible to polishing and are readily available in Tennessee. It is necessary to investigate the frictional properties of limestone-based RAP. Therefore, the laboratory-produced RAP was fabricated using four types of limestone and PG 64-22 binder with a 5.5% asphalt content. Four types of limestone aggregates were oven-dried at 105°C to a constant mass and then cooled to room temperature before screening. As shown in Figure 3-7, laboratory-produced RAP was left in the 85°C oven for 120 hours (5 days) to simulate the long-term aging over the service life of pavement [22, 23]. Consequently, laboratory-produced RAP is an artificially aged material that replicates the characteristics of real RAP after long-term pavement service.



Figure 3-7 Laboratory preparation of RAP.

3.4.3 Asphalt mixtures collection

As shown in Table 3-2, 9 types of asphalt mixtures from four regions in Tennessee were collected to evaluate their frictional properties. The primary aggregate type in each asphalt mixture is determined based on the proportion of coarse aggregates used. Traditionally, asphalt mixtures are compacted into slab specimens, which have been widely used for laboratory testing. However, this fabrication method requires a large quantity of material and specialized compaction equipment, such as a rolling wheel compactor, making the process more resource-intensive and less practical for routine evaluations. To develop a more cost-effective and convenient laboratory testing method, asphalt mixtures compacted using the Superpave gyratory compactor (SGC) were explored for skid resistance measurements. The SGC offers several advantages, including reduced material requirements, easier handling, and broader accessibility in laboratory settings, making it a viable alternative for evaluating pavement friction performance efficiently.

Table 3-2 Collected plant mixtures used for laboratory tests.

<i>Region</i>	<i>TDOT No.</i>	<i>Mixture Type</i>	<i>Main Aggregate Type</i>
<i>Region 1</i>	1230674	411-TLD mix, PG70-22	Granite
	1230715	411-D mix, PG70-22	Gravel +Slag
<i>Region 2</i>	2230203	411-D mix, PG70-22	Hard Limestone (Region3 Type II, Limestone #3)
	2230259	411-TLD, PG64/67-22	Hard Limestone (Region3 Type IV, Limestone #2)
	2230260	411-D mix, PG64/67-22	Hard Limestone (Region3 Type IV, Limestone #2)
<i>Region 3</i>	3232097	411-OGFC mix, PG76-22	Hard Limestone (Type II)
	3230061	411-D mix, PG64/67-22	Hard Limestone (Region3 Type II Limestone #3)
<i>Region 4</i>	4230043	411-D Mix, PG70-22	Gravel
	4230095	411-D Mix, PG76-22	Gravel (Region3 Gravel #2)

3.4.4 Sample fabrication

The size of the prepared slab is 500mm × 400mm × 50mm, compacted by roller compactor, as shown in Figure 3-8. The design schematic of test rings was developed by AutoCAD illustrated in Figure 3-9. The different specimens are shown in Figure 3-10. The circular path (perimeter) for CTM and DFT is 11.2 in. (284mm), and the diameter of the ring is 17.2 inch (437mm), therefore, seven gyratory pills were prepared to fabricate a test ring following the Indiana specifications [24].

The Specific procedure is listed as follows:

- (1) The target air void of SGC samples is 7%-8% (dense-graded mixtures) and the height is 80mm.

(2) Four SGC samples were sawed in half to prepare seven gyratory pills. The vertical sides of the gyratory pills should be cut at a slight angle to allow them to fit together according to Figure 3-9. (to fit the path of TWPD, DFT, and CTM).

(3) The seven gyratory pills were fitted with a metal ring clamp, placed in the center of the wooden mold.

(4) Self-leveling cement was poured into the mold to provide a flat surface for the test.

(5) The cut surface of the gyratory pills was positioned at the bottom, while the compacted surface (uncut) was designated for friction measurement.



Figure 3-8 Heated asphalt roller compactor.

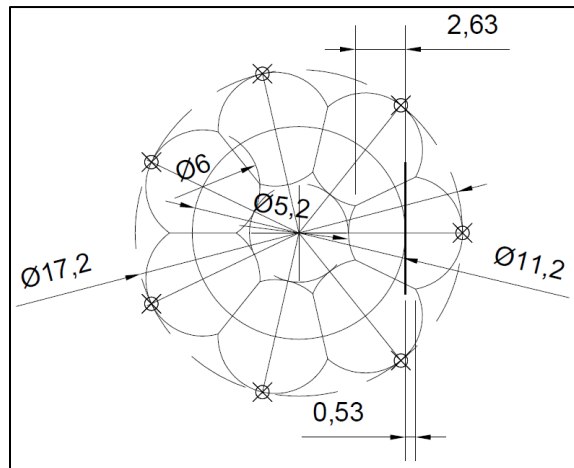
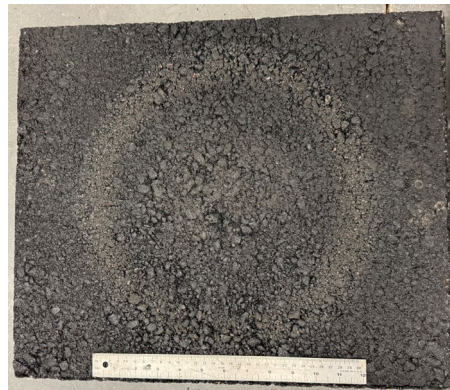


Figure 3-9 Design schematic of test ring.



Ring-shaped specimen



Slab specimen

Figure 3-10 Fabrication of ring-shaped and slab-based specimens.

3.5 Frictional performance tests

Laboratory accelerated polishing tests are essential for evaluating the long-term skid resistance of asphalt mixtures under controlled conditions. These tests simulate the effects of traffic-induced polishing within a shorter timeframe to assess the frictional performance efficiently. By subjecting asphalt specimens to accelerated polishing, the terminal wet skid resistance (the lowest friction level of pavement) can be determined in the lab. Understanding this value is crucial for predicting long-term performance and planning effective maintenance strategies. The

following sections provide details on the polishing and friction measurement procedures applied to evaluate the skid resistance of the prepared asphalt specimens.

3.5.1 Polishing device

The three-wheel polishing device (TWPD), developed by NCAT, was used to simulate the traffic-polishing effects for long-term pavement friction investigation. As shown in Figure 3-11, TWPD operated under controlled conditions with a 146 lb carriage weight, a 60 rpm (revolutions per minute) rotational speed, and the Kenda tire inflated to 35 psi. During the polishing process, the continuous water flush was applied on the asphalt mixture surface. The optical sensor was used to track the polishing cycle, where one polishing cycle corresponds to a 360-degree revolution of the three-wheel carriage, running in a counterclockwise direction [25]. To ensure consistent testing conditions, the tire is replaced when the surface texture is visibly worn, and the tire pressure is checked before each operation, as depicted in Figure 3-11.

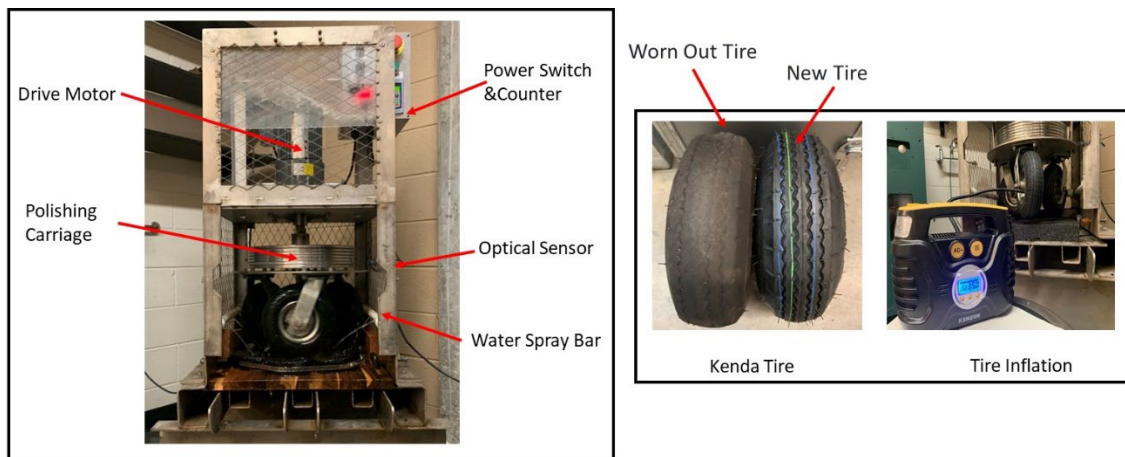


Figure 3-11 Three-wheel polishing device.

The slab-based and ring-shaped specimens were polished through 10 stages for a frictional performance test. Detailed polishing cycles are listed in Table 3-3. At the end of each cycle period, the polishing device was stopped, and the specimen was removed for relative frictional tests. A cumulative cycle of 150,000 was chosen to investigate the long-term friction deterioration trend and to reach a terminal surface friction condition. Figure 3-12 illustrates the polishing processes for slab-based and ring-shaped specimens.

Table 3-3 Polishing revolution (cycles).

<i>Stage</i>	<i>Total passes</i>	<i>Stage passes</i>	<i>Stage duration</i>
1	0	0	-
2	1,500	1,500	25 minutes
3	5,000	3,500	59 minutes
4	9,000	4,000	67 minutes
5	20,000	11,000	3 hours

6	30,000	10,000	167 minutes (2.7 hours)
7	50,000	20,000	334 minutes (5.5 hours)
8	75,000	25,000	7 hours
9	100,000	25,000	7 hours
10	150,000	50,000	14 hours



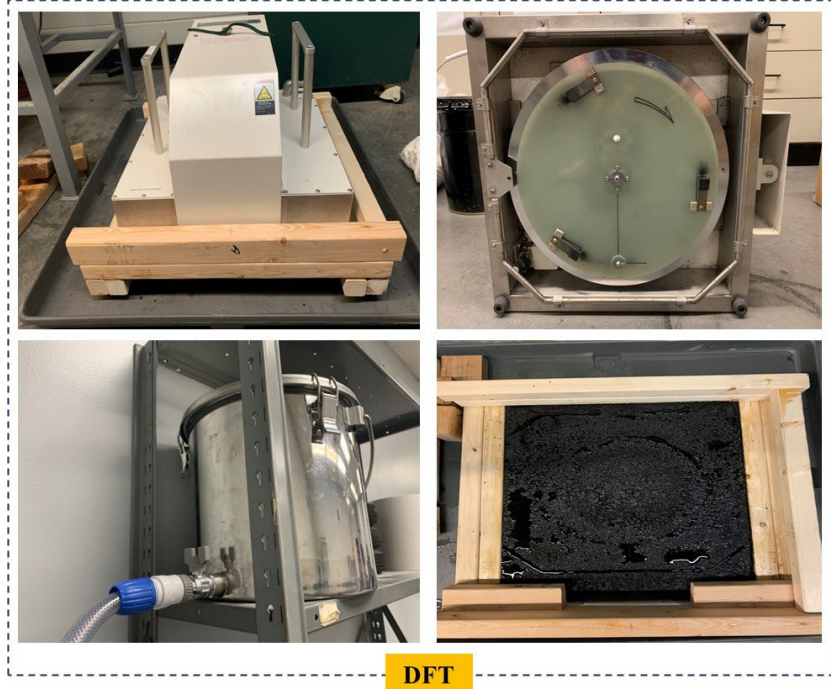
Ring-shaped specimen

Slab

Figure 3-12 Prepared specimens for polishing.

3.5.2 Dynamic friction tester

The Dynamic Friction Tester (DFT) is a portable device that is used to measure the coefficient of friction (COF) at different speeds. It consists of a rotating circular disk attached with three rubber sliders to interact with the pavement surface. The disk rotates at tangential velocities up to 80 km/h. Water flows over the pavement surface being tested to simulate wet conditions. The DFT measures the friction-speed relationship with speeds ranging from 0-80 km/h to evaluate the micro-texture characteristics. The DFT tests were reported at four speed levels (20km/h, 40km/h, 60km/h, and 80km/h). The coefficient of friction at 20 km/h (DFT20) is commonly used for pavement friction evaluation. As shown in Figure 3-13, a template was placed over the slab to ensure the measurements were taken at the same location. The test results were recorded at consecutive speed intervals for analysis. The final DFT value is determined by the average value from five measurements.



DFT

Figure 3-13 Indoor DFT test.

The torque generated by the slider forces is measured as the rotational velocity reduces due to the surface friction as well as calculating the COF as a function of speed. The COF is calculated by dividing the continuously measured torque force by the weight of the spinning disk. The diameter of the test track is 284 mm in Figure 3-14. The test surfaces were swept with a brush and were free of contamination, cracking, and surface defects.

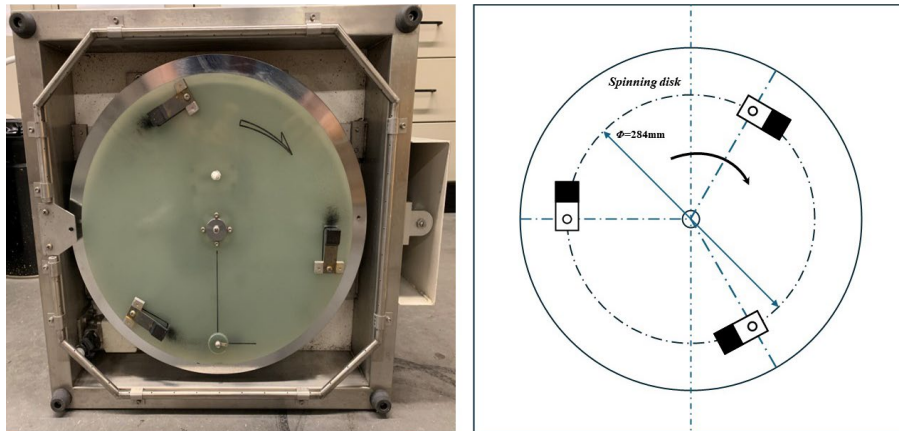


Figure 3-14 Structure sketch of DFT.

3.5.3 Circular Track Meter

Circular Track Meter (CTM) and 3D texture models were used to evaluate the pavement skid resistance. As shown in Figure 3-15, green areas indicate positive effects, such as enhanced friction for safety in dry and wet conditions. The red areas represent negative effects, such as increased tire wear, vehicle wear, noise, and reduced ride comfort. Pavement friction is

determined by both micro-texture and macro-texture while macro-texture controls the pavement friction at high speeds, as defined by the Permanent international Association of Road Congress (PIARC). Texture wavelengths below 0.5 mm are classified as micro-texture, while wavelengths ranging from 0.5 mm to 50 mm are considered macro-texture. Micro-texture is essential for dry weather friction, as it provides direct tire-surface contact. Macrotexture is more important for wet weather friction, allowing water drainage from the surface to reduce hydroplaning risks. Macrotexture also impacts splash and spray, which affects visibility in wet conditions. The balance between texture types is essential to optimize both safety (friction) and comfort (ride quality and noise).

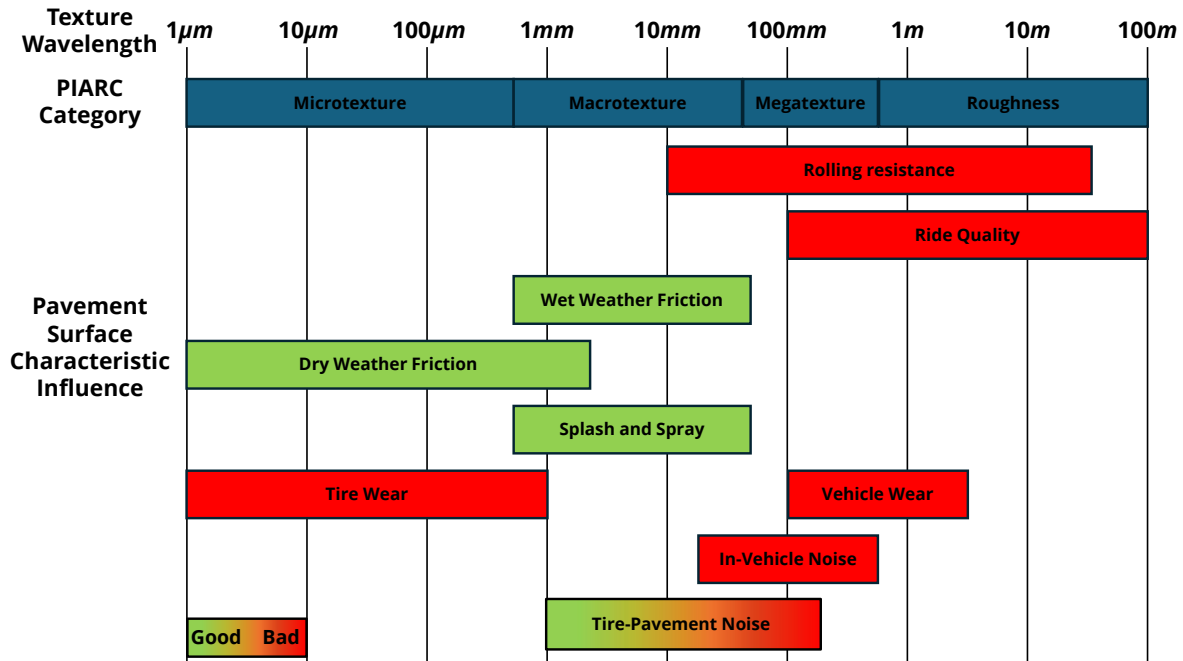


Figure 3-15 World Road Association (PIARC) texture definitions and their influence on pavement surface characteristics [26].

Mean profile depth (MPD) is a type of macro-texture index tested by Circular track meter (CTM) shown in Figure 3-16. As shown in Figure 3-16, multiple directions of data can be obtained in one measurement, i.e., driving direction, perpendicular to the direction of travel, 45° to the direction of the travel, and the whole circumference. The circular diagram is divided into eight segments (A to H), with measurements taken at 45° intervals. Segment C and G are perpendicular to the direction of travel, representing the texture along the vehicle's travel path during field testing. The radius of the circumference is 142 mm and a total of 1024 samples are tested during one measurement period. The profile height of 8 segments is utilized to calculate MPD.

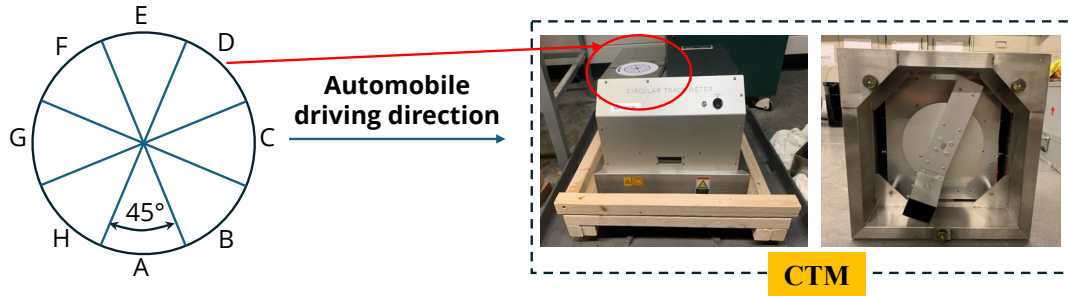


Figure 3-16 Indoor pavement texture test via CTM.

The average of eight segments, referred as the MPD, was then compared to the base length of 100 mm in the specification [27]. MSD and MPD were calculated using Equation (3-1) and Equation (3-2),

$$MSD = \frac{1}{2} (Peak\ level^{1st} + Peak\ level^{2nd}) \quad (3-1)$$

$$MPD = \frac{1}{n} \sum_{i=1}^n MSD_i \quad (3-2)$$

where n is 8, representing the number of segments.

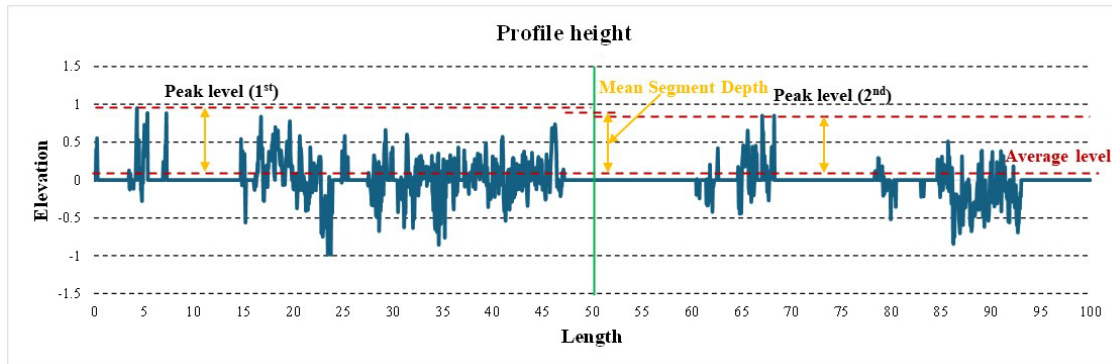


Figure 3-17 2D Profile obtained from CTM.

3.6 Field pavement skid resistance test

3.6.1 Selection of test segments

In addition to the laboratory investigation of surface texture through COF, field pavement skid resistance was assessed by evaluating both pavement micro-texture and macro-texture, as well as COF measurements. A total of 11 test segments in Tennessee were selected for the evaluation of pavement skid resistance.

3.6.2 Skid resistance test setup

As shown in Figure 3-18, the outer lane, which is subjected to heavy traffic, was selected for the pavement skid resistance test. This lane typically experiences higher traffic volumes, including heavy vehicles such as trucks, which contribute to increased surface polishing over time, making it representative of the worst-case scenario for skid resistance. Testing under these conditions

ensures a comprehensive assessment of pavement performance and provides a safety margin for skid resistance, helping to establish reliable maintenance strategies.

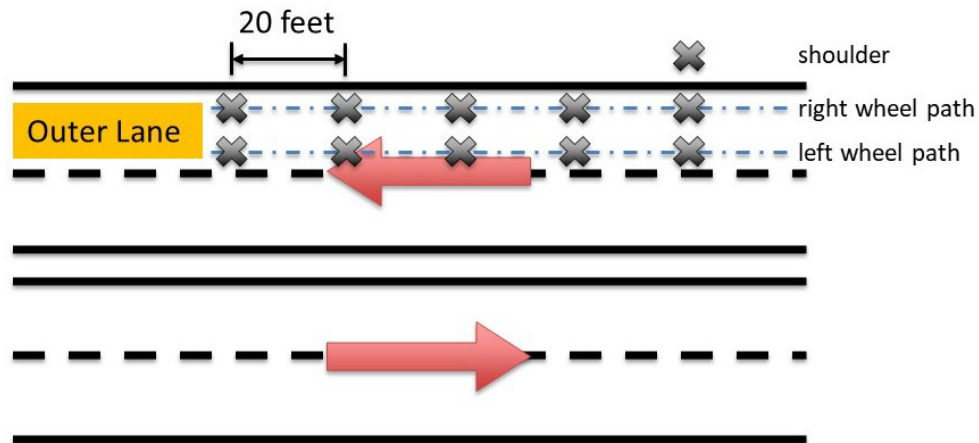


Figure 3-18 Schematic for the field pavement skid resistance test.

Comparative studies were conducted in the left wheel path, right wheel path, and the pavement shoulder, with the shoulder assumed to represent the initial skid resistance. The distance for measurement spots is 20 feet in the field. The DFT, CTM, and sand patch test (SPT) were performed to evaluate the field pavement performance, as illustrated in Figure 3-19.



Figure 3-19 Field pavement skid resistance performance test.

The sand patch test is a volume-based method used to calculate the mean texture depth (MTD), used to quantify the macrotexture of pavement surface. Sand with a specific volume is used in each test. The sand is spread with a spreading disc to create a circular patch on the pavement surface and the diameter of the circular patch is measured at four locations equally spaced around the perimeter of the patch. The MTD is expressed by Equation (3-3):

$$MTD = \frac{4V}{\pi D^2} \quad (3-3)$$

where V is the sample volume of sand (in.³), D is the average diameter of the area covered by the material (in.).

The permanent international association of road congress (PIARC) developed a unified index, the international friction index (IFI), to comprehensively evaluate the pavement skid resistance at both micro- and macro-levels expressed by Equations (3-4) and (3-5):

$$IFI = 0.081 + 0.732 \times DFT_{20} \times \exp\left(\frac{-40}{S_p}\right) \quad (3-4)$$

$$S_p = 14.2 + 89.7MPD \quad (3-5)$$

where S_p is the speed constant parameter.

3.6.3 Locked wheel skid trailer from TDOT

TDOT utilizes the locked wheel skid trailer test (LWST) for the field pavement friction test in accordance with ASTM E274 [14], as shown in Figure 3-20 and Figure 3-21. The device can measure the pavement skid resistance at traveling speeds. The equipment consists of a pickup truck, locked-wheel trailer, and water distribution systems. The tire is fully locked during the test and the slip speed of the tire is equal to the traveling speed. The horizontal friction force and the dynamic vertical load are recorded, and the skid number (friction number) is calculated as follows:

$$SN = \left(\frac{F}{W}\right) \times 100 \quad (3-6)$$

where F is the horizontal force and W is the vertical load applied to the test wheel.



Figure 3-20 Locked wheel skid trailer from TDOT.



Figure 3-21 Tire configuration of the LWST.

Skid number (SN) is measured by the LWST at different speeds and SN40 at 40 mph is commonly used for friction evaluation. SN measured with ribbed tire and smooth tire at 40mph is designed as SN40R and SN40S, respectively. An FHWA memorandum provides for federal financial assistance in correcting existing pavement surfaces that have SN less than 35 [28]. Utah DOT classified pavement friction condition into Good (SN greater than 45), Fair (ranging from 35 to 45), and Poor (SN less than 35) [29]. Adequate skid resistance is defined as a SN value greater than 35 based on practice.

Chapter 4 Results and Discussion

4.1 Analysis for aggregate skid resistance

4.1.1 Correlation between SiO₂ and PSV

Figure 4-1 shows the BPN (before polishing) and PSV (after polishing) of the tested aggregates. The friction reduction rate of aggregates varies significantly among different aggregate types and sources. It can be seen from Figure 4-1 that the minimum PSV of R3 Limestone #2 is 30, which meets the material requirements of TDOT. The rest of the tested limestone aggregates are classified as type I and Type II aggregates, which have higher PSV values and are less susceptible to accelerated polishing, thus being widely used for pavement surface construction. All the tested aggregates meet the minimal PSV requirements.

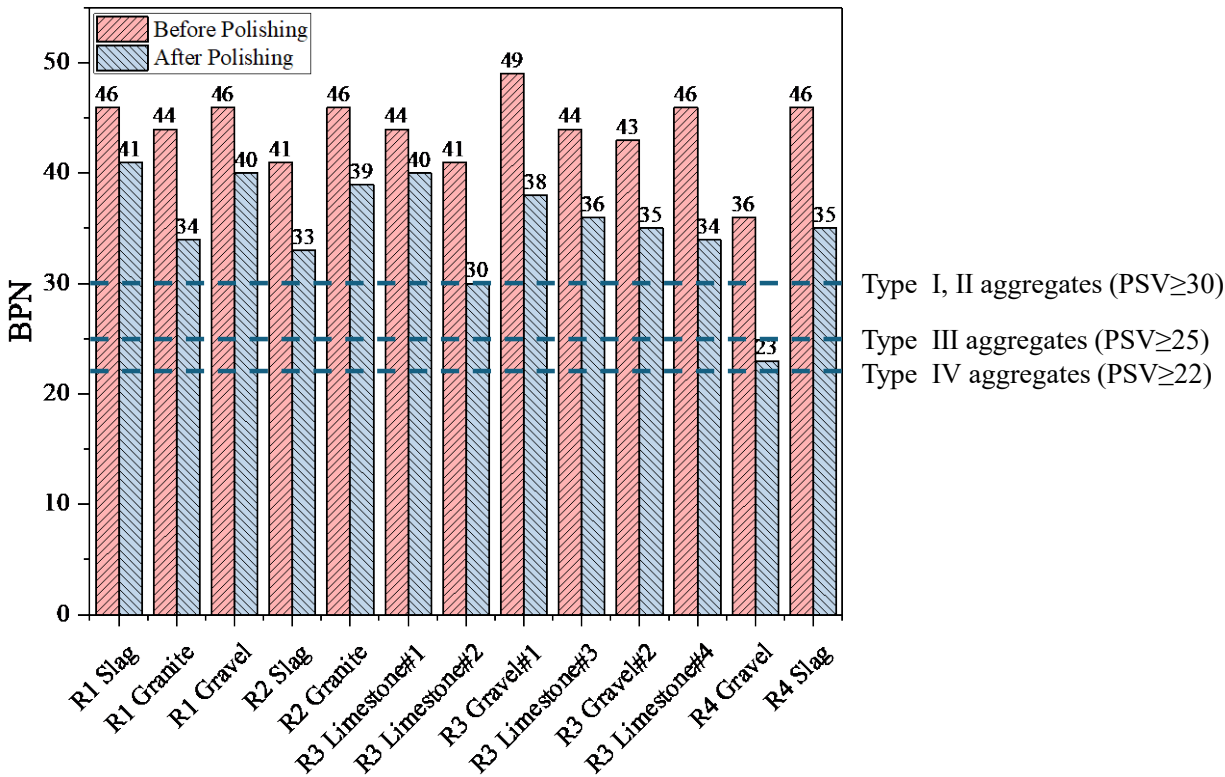


Figure 4-1 Polishing-resistant performance comparison before and after polishing.

Compared with other types of aggregates, limestone is more prone to losing micro-textural frictional performance due to polishing [30]. The percentage of SiO₂ content in aggregates provides an insight into frictional properties. To determine the qualified limestone material for pavement construction, it is important to correlate the chemical composition (such as SiO₂ and CaO contents) with the PSV. Four sources of limestone in Region 3 were chosen for regression analysis to correlate the PSV with SiO₂ content to give insights into a quick frictional evaluation. Chemical compositions of aggregates were tested with selected sizes to ensure uniformity. The SiO₂ and CaO contents of the tested limestone are shown in Figure 4-2. As the size of the particle decreases, the content of SiO₂ and CaO increases due to the more uniformity and exposed surfaces. The same is true based on our results.

The observed variation in SiO₂ content with aggregate size is a result of the X-ray fluorescence (XRF) testing methodology rather than an actual change in the SiO₂ composition of the aggregates. XRF provides surface-level elemental composition data, and the accuracy of the measurements is influenced by the uniformity of the aggregate particles. Smaller, more uniform particles provide a larger exposed surface area, allowing for more consistent and accurate readings. In contrast, larger particles may have surface irregularities or coatings that introduce variability in the results. It is important to clarify that this does not mean the SiO₂ content of the aggregates changes with particle size; rather, it varies in the XRF test results due to differences in particle surface characteristics and uniformity.

Aggregates retained on 1/2 in. and 3/8 in. present higher standard deviation when used for SiO₂ test while finer aggregate size exposes more surfaces and test results are more reliable on this basis. In Figure 9, SiO₂ and CaO contents of aggregates retained on No.4 (4.75mm) are close to those retained on No.8 (2.36mm). The standard deviation is acceptable for engineering applications. Coarse aggregates contribute to pavement skid resistance and the American Society for Testing and Materials (ASTM) defines aggregates retained on No.4 (4.75mm) size as coarse aggregates. Therefore, the results of No.4 aggregates can be representative parameters for polish resistance evaluation to minimize the influence of aggregate size and surface irregularities. There is no need to screen the fine aggregates, especially for asphalt pavement with coarse aggregate size. The final SiO₂ and CaO contents of No.4 aggregates are used for PSV correlation.

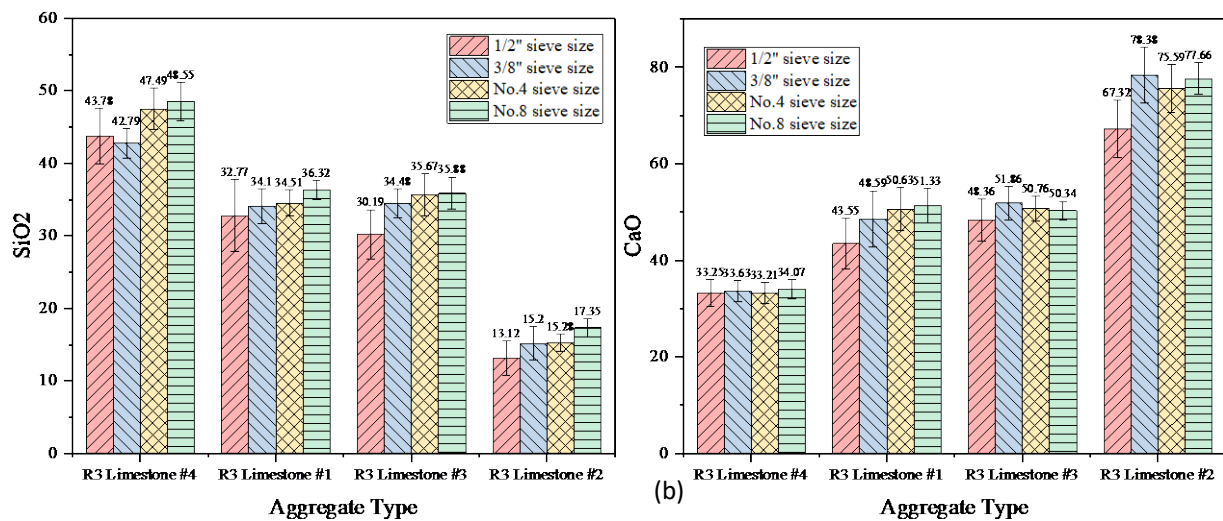


Figure 4-2 Chemical composition in limestones: (a) SiO₂ content in limestone; and (b) CaO content in limestone.

Based on frictional properties and chemical composition of four types of limestones in Region 3, both linear and polynomial fit were used to derive regression for statistical analysis to better fit the test data. Figure 4-3 describes the relationship between PSV and chemical composition content. From Figure 4-3(a), it is noted that the R² between SiO₂ and PSV for linear regression and polynomial regression are 0.81, and 0.89 respectively. Polynomial regression performs better than the linear fit based on the results. Despite the presence of outliers in both the linear and polynomial regression models, the very low p-values (3.83×10^{-7} and 7.79×10^{-8}), which are well below the significance threshold of 0.01, indicate a strong statistical significance. The result in

Figure 4-3(a) means aggregates become more polish-resistant as SiO_2 increases, proven to be a good indicator for frictional properties.

As shown in Figure 4-3(b), the R^2 values for both linear and polynomial regression models (0.28 and 0.57, respectively) indicate a weak goodness of fit. This demonstrates that lower CaO content does not necessarily imply higher SiO_2 content in aggregates, and consequently, does not guarantee improved frictional properties. Since SiO_2 is the primary contributor to polishing resistance, CaO content alone cannot be used as a reliable predictor of skid resistance.

Therefore, silica-abundant aggregates facilitate the improvement of pavement skid resistance. Qualified aggregates or RAPs could be selected based on polynomial regression. Based on the results, it can be inferred that aggregates should contain at least 25% SiO_2 to achieve a PSV greater than 30.

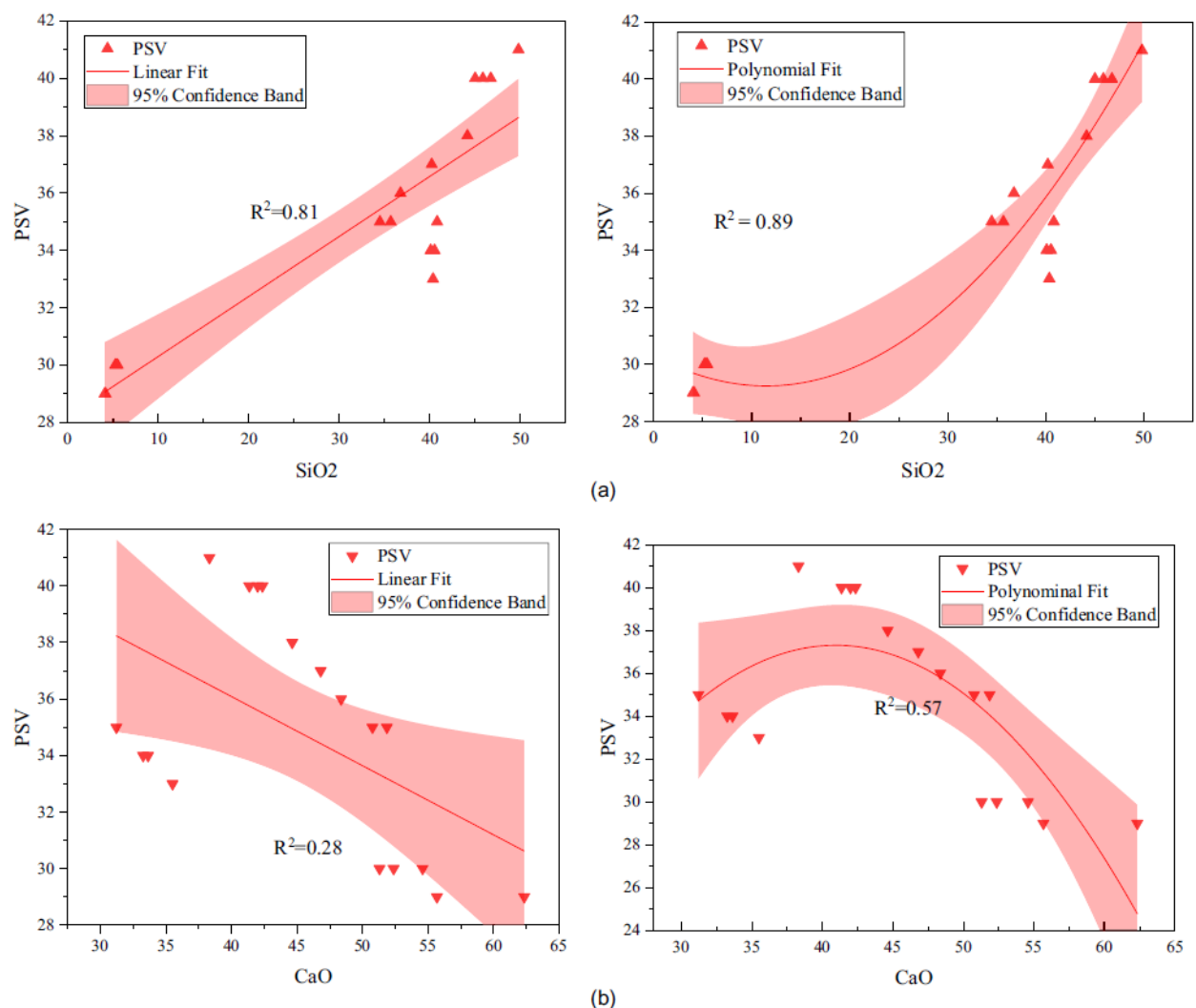


Figure 4-3 Correlation between PSV and chemical composition: (a) correlation between SiO_2 and PSV; and (b) correlation between CaO and PSV.

4.1.2 Correlation between SiO₂ and Micro-Deval test

The MD test is a substitute for frictional property evaluation. Therefore, the relationship between SiO₂ and MD abrasion loss can evaluate the frictional properties to some extent. As shown in Figure 4-4(a), limestone provides less abrasion resistance compared with gravel and granite. Type II limestone shows better abrasion resistance than type IV limestone. The MD loss value should be less than 17 to 20 percent to provide sufficient frictional resistance [31]. Therefore, all tested aggregates are qualified to provide acceptable skid resistance.

Figure 4-4(b) describes the relationship between MD loss and PSV based on linear regression. It is noted that aggregates with lower Micro-Deval loss present higher PSV, thus providing higher pavement skid resistance based on the tendency. Region 3 limestone#2 has the highest MD loss which results in the lowest PSV, which means the MD loss can be used as an alternative method to evaluate the polish resistance. Figure 4-4(b) presents the correlation between MD loss and SiO₂ with an R^2 of 0.60. The p-value is 0.015 lower than 0.05 and the fit is still statistically significant. Therefore, the SiO₂ content can reasonably represent the abrasion and polishing resistance to some extent to help understand the frictional properties of aggregates as well as asphalt mixtures.

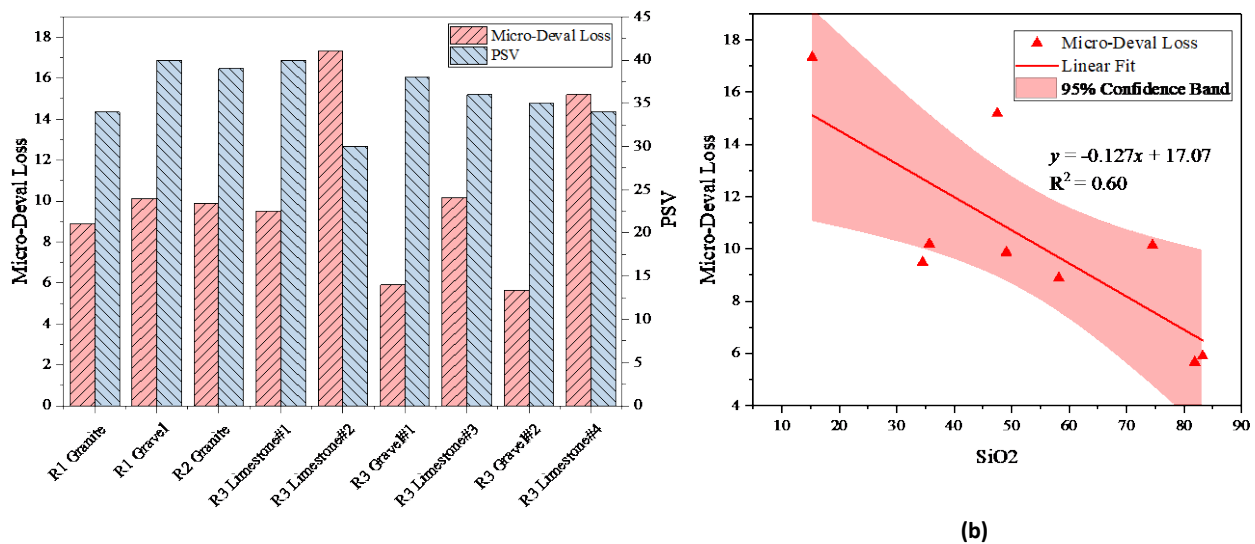


Figure 4-4 MD abrasion loss results: (a) correlation between MD loss and PSV; and (b) correlation between MD loss and SiO₂.

4.1.3 Correlation between SiO₂ and AIMS test

Figure 4-5 shows the image-based aggregate surface evaluation indicators measured by AIMS, including the commonly used angularity index and texture index. The morphological characteristics of aggregates were accurately measured by AIMS. Table 4-1 lists the angularity index and texture index values before and after the MD abrasion test. It is observed that most of the limestones present higher initial angularity and texture properties compared to gravel and granite, primarily due to the crushing process.

It is indicated that slag exhibits higher abrasion resistance compared to other materials. This is evidenced by its lower angularity and texture index loss percentages after the MD test. In both Region 1 and Region 2, slag demonstrates lower percentage losses in both angularity and texture

indices, suggesting its superior ability to retain surface characteristics. These results confirm that slag is a more durable aggregate choice for maintaining long-term pavement friction.

Based on Figure 4-5, it is noted that the angularity of all the tested aggregates ranges from 2100 to 3975, which is classified as moderate angularity. As for the texture index, granite presents more rough surface characteristics with a moderate texture index. However, limestone has a greater texture index before abrasion while showing an inferior performance after abrasion. The relationship between SiO₂ content and the image-based surface index is shown in Figure 4-5.

Table 4-1 AIMS results.

<i>Region</i>	<i>Material</i>	<i>Angularity index</i>			<i>Texture index</i>		
		Before MD	After MD	Loss (%)	Before MD	After MD	Loss (%)
<i>Region1</i>	Granite	3,101.2	2,571.7	17.07	348.4	227.0	34.85
	Gravel	2,964.5	2,123.9	28.36	197.3	181.2	8.16
	Slag	4,499.5	3644.0	19.01	399.9	345.6	13.58
<i>Region2</i>	Granite	2,602.8	2,084.1	19.93	533.5	486.3	8.85
	Slag	3689.1	3119.9	15.43	351.4	323.5	7.94
<i>Region3</i>	Limestone#1	3,001.2	2,135.1	28.86	327.4	166.7	49.08
	Limestone#2	2,566.5	2,065.9	19.51	265.2	119.7	54.86
	Gravel#1	3,170.2	2,594.6	18.16	175.8	169.3	3.70
	Limestone#3	3,309.4	2,408.7	27.22	311.4	166.5	46.53
	Gravel#2	3,117.4	2,543.3	18.42	178.7	165.8	7.22
	Limestone#4	3,092.5	2,347.9	24.08	278.2	203.4	26.89

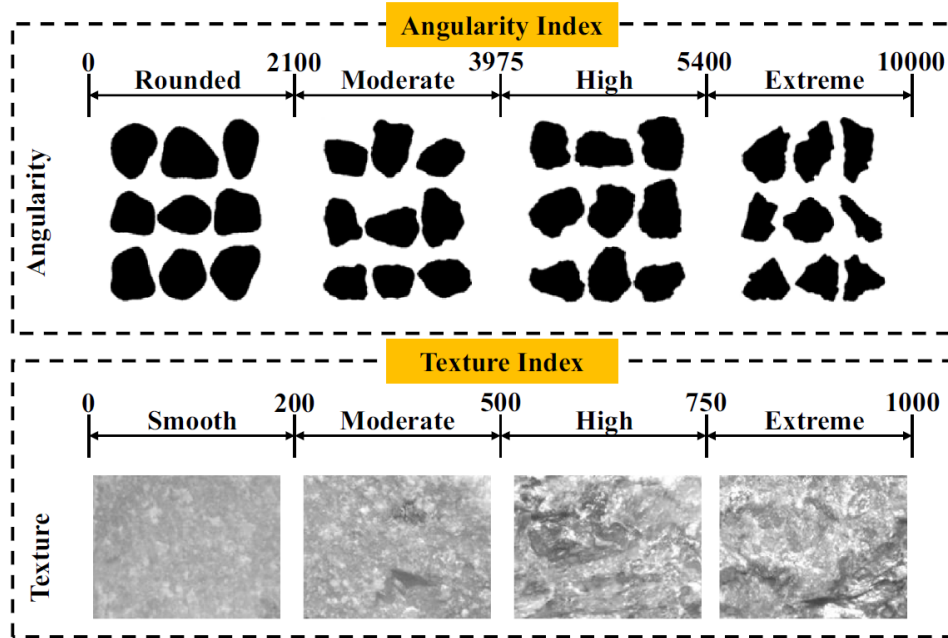


Figure 4-5 Image-based evaluation metrics.

Figure 4-6(a) describes the relationship between angularity loss and SiO₂ content based on linear regression. The R^2 between angularity loss and SiO₂ is 0.41, although it is not significant for analysis. It can be noticed that with the increase of SiO₂, the angularity loss will decrease to some extent. As for texture loss, Figure 4-6(b) depicts that the texture loss is strongly correlated with the SiO₂ contents of aggregates and SiO₂-abundant aggregates show smaller texture loss. Therefore, once obtained with the SiO₂ of aggregates or asphalt mixtures, the overall skid resistance can be estimated based on the regression model. In addition, more sources of aggregates need to be investigated in the future for a better understanding of relationship between texture loss and SiO₂ contents.

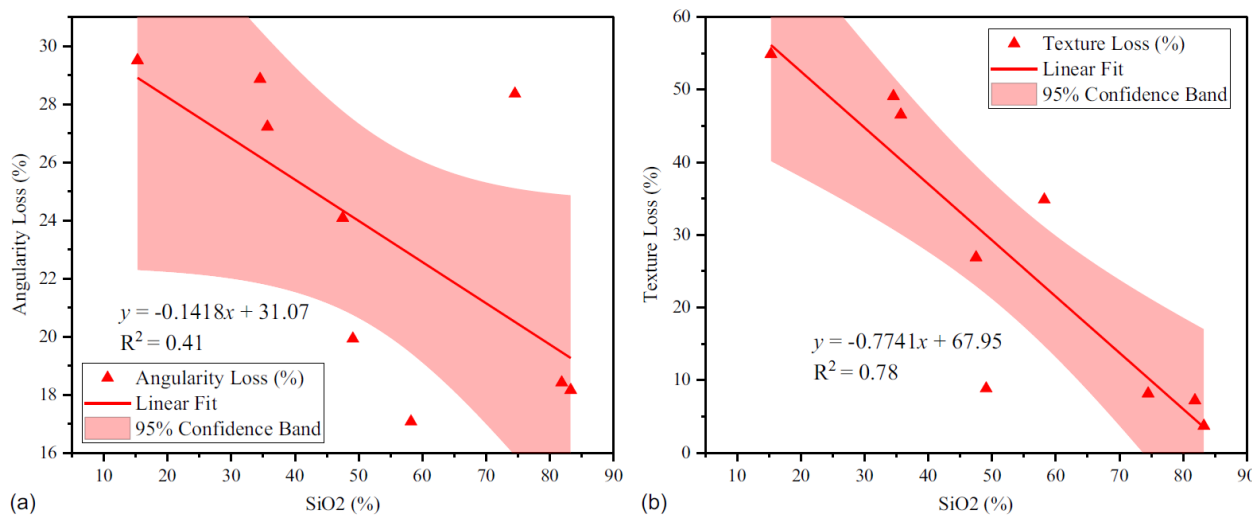


Figure 4-6 Angularity and texture change with different SiO₂ contents: (a) correlation between angularity loss and SiO₂; and (b) correlation between texture loss and SiO₂.

4.1.4 SiO₂ content of RAP

The SiO₂ content of laboratory-produced RAP is shown in Figure 4-7. Compared with Figure 4-2, the SiO₂ content of laboratory-produced RAP (no processing) is much lower than that of original aggregates because of the influence of asphalt. The asphalt binder influences the penetration of X-ray into the aggregate surface, which decreases the SiO₂ content of test results. As shown in Figure 4-7, the SiO₂ of original aggregates without asphalt is presented. It is noted that the SiO₂ of RAP without processing remains half of that of original aggregates. Additionally, the standard deviation of that is higher than the original aggregates due to the asphalt binder.

There are two primary methods to remove asphalt binder from RAP: chemical dissolution and ignition testing. However, the ignition method, which involves exposing the material to high temperatures, can lead to the thermal decomposition of aggregates, potentially compromising the accuracy of SiO₂ content measurements. In contrast, chemical dissolution using Trichloroethylene (TCE) provides a more reliable approach by effectively dissolving the asphalt binder without affecting the aggregate properties. Therefore, TCE was chosen for processing laboratory-produced RAP to ensure precise and accurate SiO₂ content evaluation.

Laboratory-produced RAP was treated with different washing times to identify the most suitable and practical approach for measuring SiO₂ content. It is noticed that the SiO₂ content is significantly influenced by asphalt in Figure 4-7. When laboratory-produced RAP was processed by TCE once, the SiO₂ contents were close to the virgin aggregates. However, the unclean aggregate surfaces are the reason that they exhibit a substantial variance. Laboratory-produced RAP treated by TCE twice shows higher SiO₂ contents while they are not accurate enough. The treated laboratory-produced RAP presents close contents to the virgin aggregates when washed by TCE three times. Most of the asphalt binder could be removed by TCE for the first time and SiO₂ contents increased dramatically compared to the laboratory-produced RAP with no processing. On this basis, field-sampled RAP can be processed by TCE to effectively remove asphalt binders to quantify the SiO₂ content of aggregates.

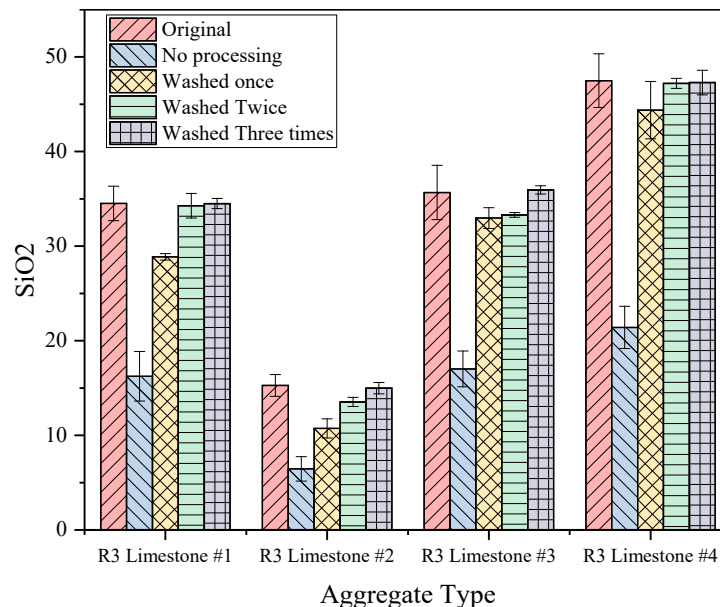


Figure 4-7 SiO₂ of laboratory-produced RAP with different treatments.

In addition to the chemical solution treatment, physical treatment using the hammer was used to expose the aggregate surfaces. Aggregates retained on 1/2 in. (12.5 mm) and 3/8 in. (9.5 mm) sieves were crushed by a hammer to screen aggregates retained on No.4 size to test the SiO₂ content. It should be emphasized that the crushed aggregate surface should be positioned facing the X-ray emitter to directly receive the X-ray for accurate measurement of SiO₂ content. Table 4-2 describes the SiO₂ of crushed laboratory-produced RAP by a hammer, providing a cost-effective method to measure SiO₂ content in RAP quickly.

The analysis can be conducted on RAP materials obtained from different pavement layers, including surface, base, and subbase layers, to provide a comprehensive evaluation of RAP properties. A more general testing method can be applied to account for variations in RAP sources. Although the majority of RAP originates from surface pavement constructed according to TDOT material specification standards, which include the use of aggregates meeting minimum silica dioxide requirements, variations in aggregate sources and mix designs may still exist. Additionally, since RAP mixtures often contain a combination of polish-resistant aggregates and polish-susceptible aggregates, this approach allows for improved control and evaluation of the collected RAP.

The measured SiO₂ content of the crushed laboratory-produced RAP is close to that of virgin aggregates for four types of aggregates in Table 4-2. In comparison to the TCE-treated method, crushing the aggregates offers a fast and straightforward approach to measuring chemical composition. It is noted that the R3 Limestone #2 aggregate has the lowest SiO₂ content with the highest texture loss in Table 4-1. Figure 4-6(b) demonstrates a strong correlation between texture loss and the SiO₂ content. The confidence band for Figure 4-6(a) is wide with respect to angularity loss and the correlation between SiO₂ content and angularity loss is not that strong enough. It is therefore that even with the lowest SiO₂ content, R3 Limestone #2 aggregate presents the highest texture loss while it does not show the highest angularity loss, meaning that texture is more susceptible to MD abrasion than angularity.

Table 4-2 Test results of crushed laboratory-produced RAP.

Aggregate source	SiO ₂ (%)	
	Virgin aggregates	Crushed RAP
R3 Limestone#1	34.51	32.78
R3 Limestone#2	15.28	13.20
R3 Limestone#3	35.67	35.17
R3 Limestone#4	47.49	43.78

It is worth noting that the results treated by TCE exhibit a smaller standard deviation compared to those treated by the hammer. All these field-sampled RAPs were screened on the No.4 sieve for the XRF test. The proper explanation is that the larger aggregates, which are distinct from those retained on the No. 4 sieve, were crushed using the hammer for the test. Consequently,

tested crushed aggregates are different from the original smaller aggregates. However, aggregates treated by TCE are more uniform, resulting in a lower standard deviation compared with those processed by the hammer. Thus, the SiO₂ content measured from field-sampled RAP treated by TCE can provide more reliable and consistent results.

Table 4-3 SiO₂ contents of field-sampled RAP.

Sample number	SiO ₂ content (%)		
	Without processing	Washed three times by TCE	Crushed by a hammer
RAP_1	15.18	25.37	20.75
RAP_2	16.57	24.33	23.66
RAP_3	15.86	25.03	29.32
RAP_4	18.53	23.52	24.33
RAP_5	20.66	28.77	26.75
Mean	17.36	25.40	24.36
Standard deviation	2.23	2.01	3.42

4.2 Analysis of laboratory asphalt mixtures

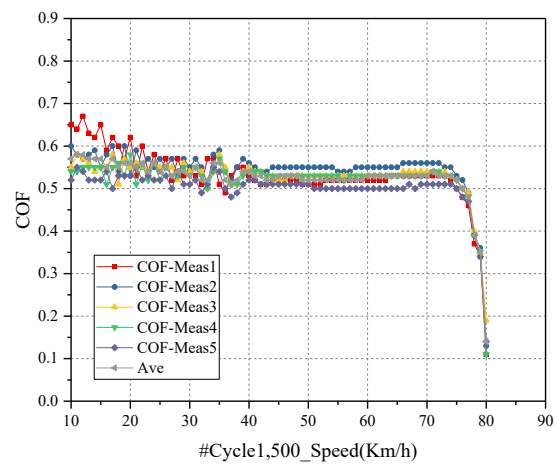
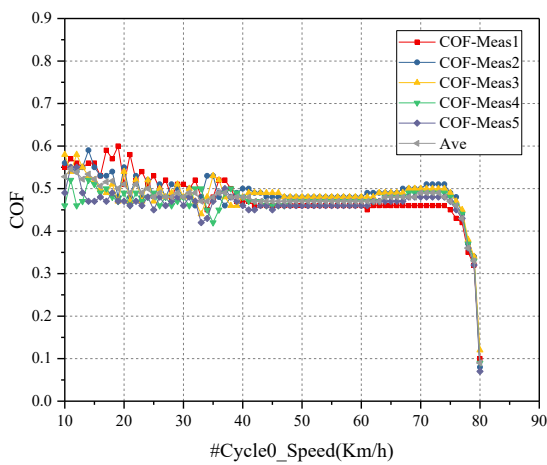
4.2.1 Comparison between slab-based and ring-shaped specimens

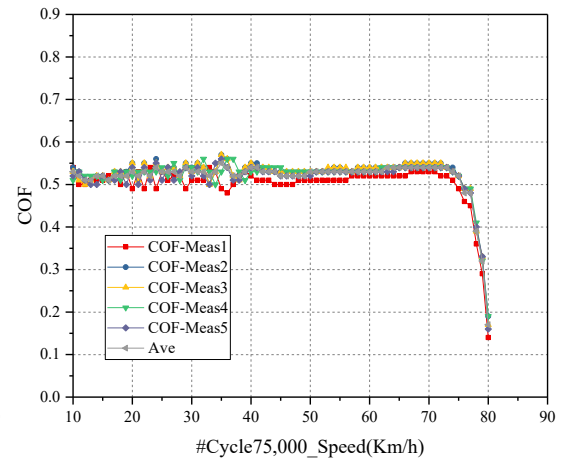
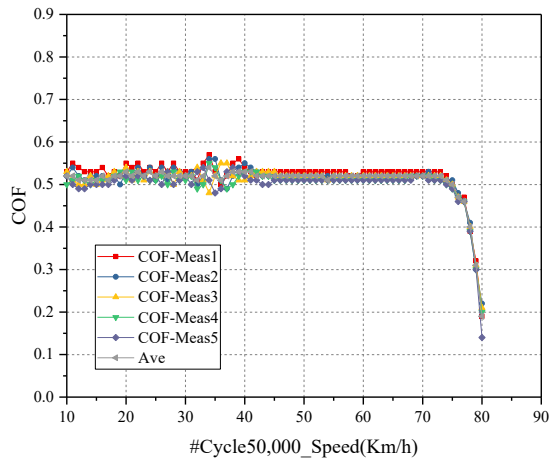
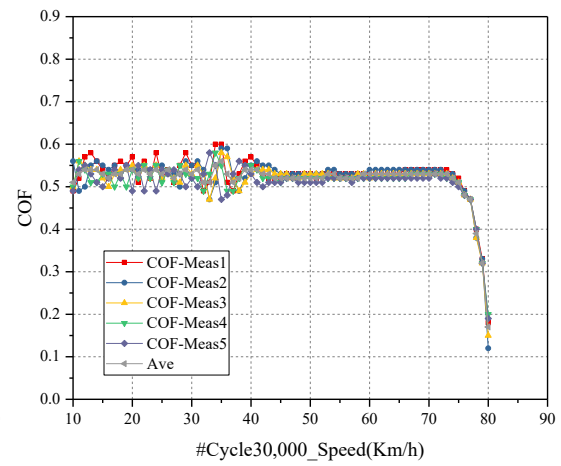
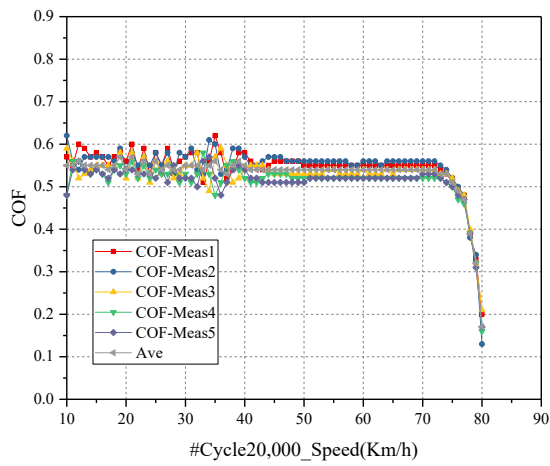
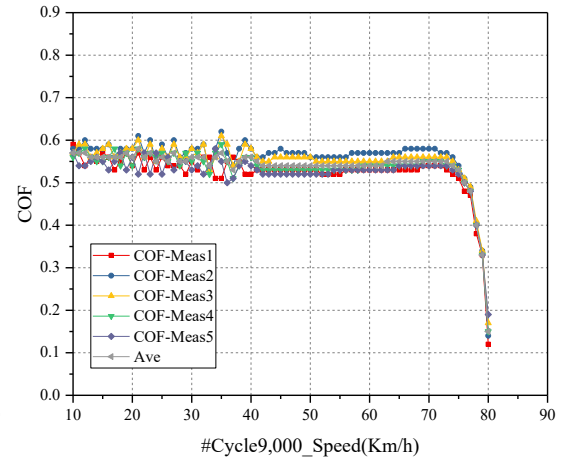
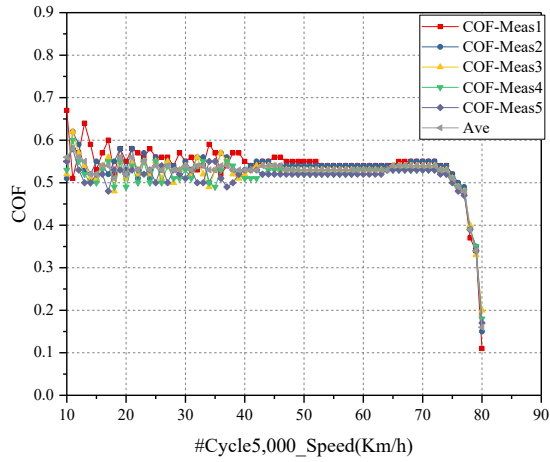
The asphalt mixture from Region 1 (No.1230674) was fabricated into both slab and ring-shaped specimens for comparative analysis. Table 4-4 and Table 4-5 list the COF tested by DFT for slab and ring-shaped specimens respectively.

Table 4-4 Results of slab-based asphalt mixture specimen.

Cycles	Speed (km/h)	DFT results	Cycles	Speed (km/h)	DFT results
0	10	0.53	30,000	10	0.51
	20	0.51		20	0.54
	40	0.48		40	0.55
	60	0.47		60	0.53
	80	0.09		80	0.17
1,500	10	0.57	50,000	10	0.52
	20	0.56		20	0.53
	40	0.54		40	0.53
	60	0.53		60	0.52

	80	0.14		80	0.19
5,000	10	0.56	75,000	10	0.53
	20	0.52		20	0.53
	40	0.53		40	0.54
	60	0.53		60	0.53
	80	0.16		80	0.17
9,000	10	0.57	100,000	10	0.5
	20	0.56		20	0.5
	40	0.56		40	0.52
	60	0.54		60	0.51
	80	0.15		80	0.16
20,000	10	0.55	150,000	10	0.5
	20	0.54		20	0.49
	40	0.55		40	0.49
	60	0.54		60	0.5
	80	0.17		80	0.15





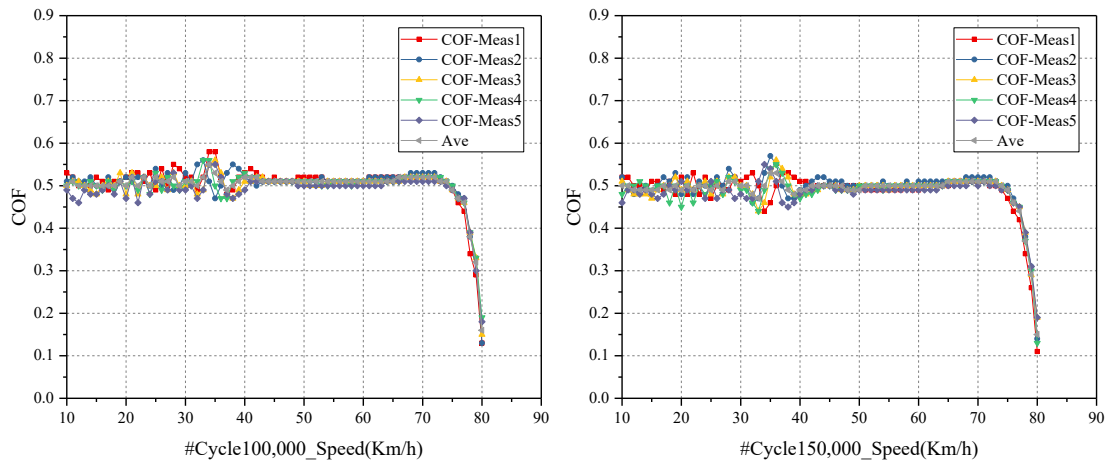


Figure 4-8 DFT results of five replicate tests during different polishing cycles based on slab specimens.

COF measured by DFT at different polishing cycles is shown in Figure 4-8. It is noticed that measured μ (COF) is stable from speed 40km/h to 70km/h. Figure 4-8 shows that DFT80 has higher variability, which is lower than DFT20, DFT40, and DFT60. At a high speed of 80 km/h, the influence of micro-texture on pavement friction diminishes significantly, making macro-texture the dominant factor in determining skid resistance.

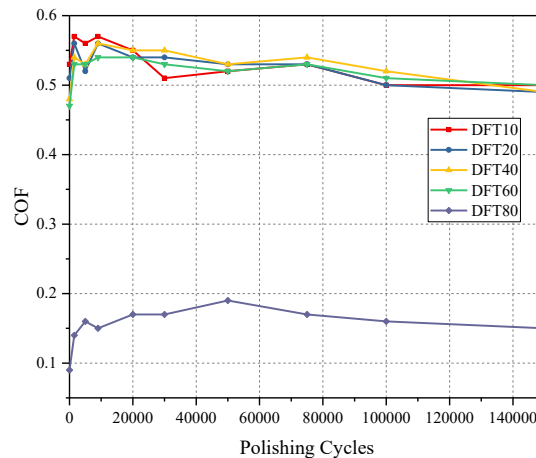


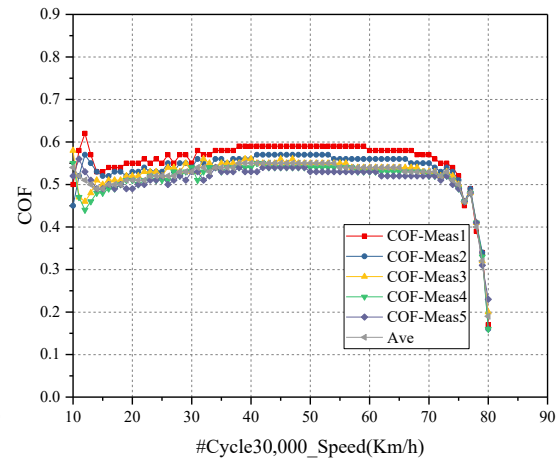
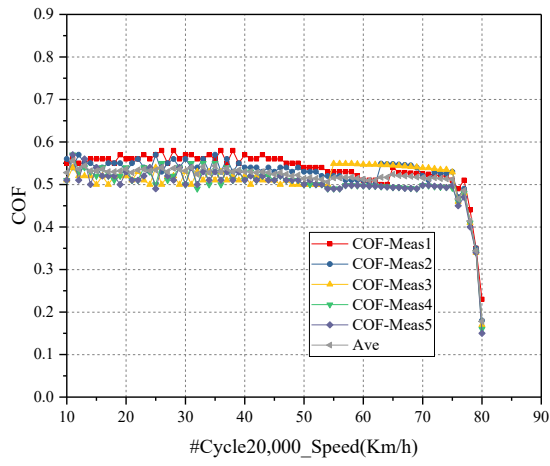
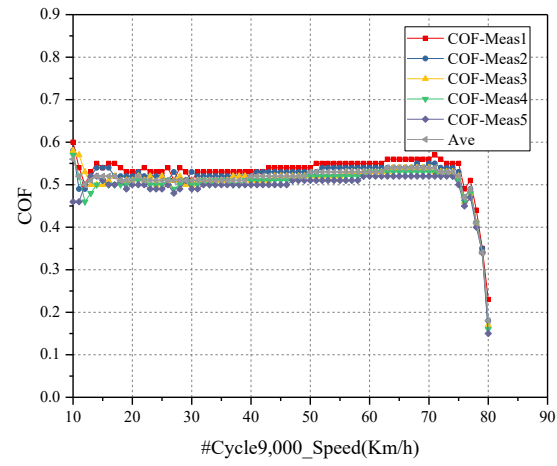
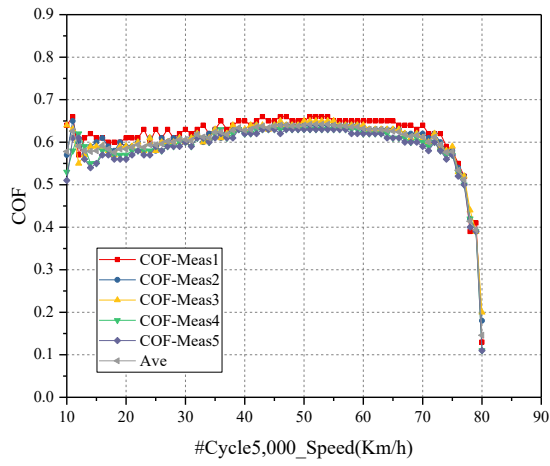
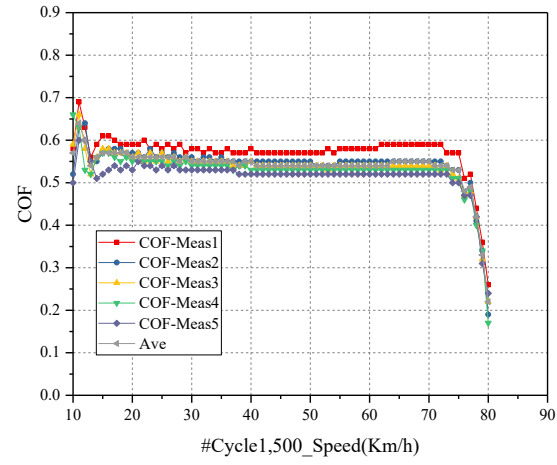
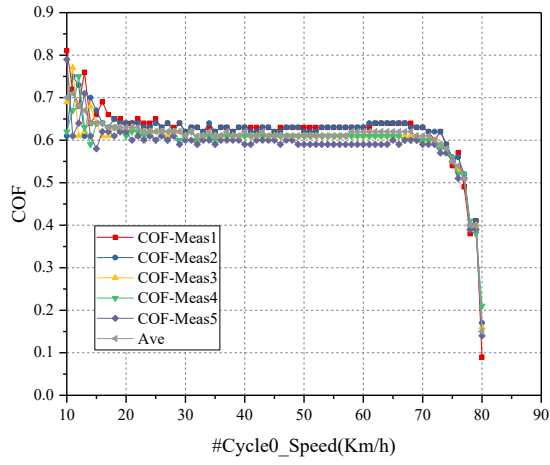
Figure 4-9 DFT changes on slab with incremental polishing cycles.

It can be seen from Figure 4-9 that the coefficient of friction reaches peak friction before the 10,000 polishing cycles and then it decreases with incremental polishing cycles. The coefficient of friction initially increases as the asphalt film wears off, then decreases due to aggregate polishing, and eventually stabilizes at approximately 0.5 except DFT80.

Table 4-5 Results of ring-shaped asphalt mixture specimen.

Cycles	Speed (km/h)	DFT results	Cycles	Speed (km/h)	DFT results
0	10	0.61	30,000	10	0.54
	20	0.62		20	0.51

	40	0.60		40	0.55
	60	0.59		60	0.54
	80	0.14		80	0.19
<i>1,500</i>	10	0.57	50,000	10	0.54
	20	0.56		20	0.53
	40	0.55		40	0.53
	60	0.54		60	0.54
	80	0.22		80	0.13
<i>5,000</i>	10	0.58	75,000	10	0.54
	20	0.58		20	0.52
	40	0.63		40	0.57
	60	0.53		60	0.54
	80	0.15		80	0.13
<i>9,000</i>	10	0.56	100,000	10	0.51
	20	0.51		20	0.51
	40	0.52		40	0.52
	60	0.53		60	0.53
	80	0.18		80	0.16
<i>20,000</i>	10	0.53	150,000	10	0.53
	20	0.54		20	0.50
	40	0.53		40	0.55
	60	0.51		60	0.53
	80	0.18		80	0.18



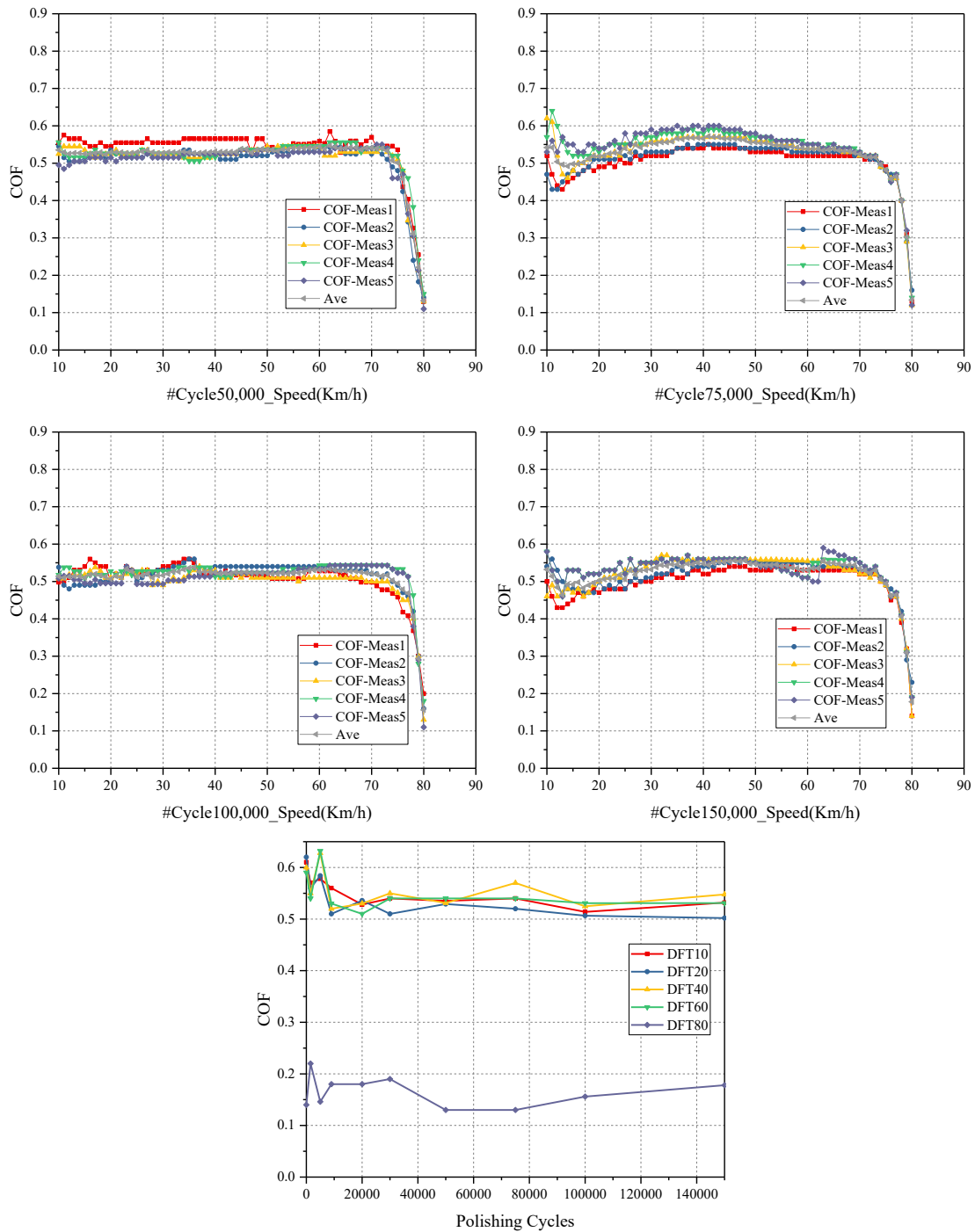


Figure 4-10 DFT changes with incremental polishing cycles based on ring specimens.

The paired t-test was employed to calculate the p-value for each polishing cycle, comparing the DFT results of slab and ring-shaped specimens. The null-hypothesis is that there is no significant difference between the two groups. The calculation is based on the paired speed DFT values from different groups. For cycle 0, it is noted that the p-value is 0.0021, showing significant difference at the beginning. However, the p-values for the rest of the polishing cycles are greater than 0.05, accepting the null-hypothesis and demonstrating that there is no significant difference between

the slab and ring-shaped specimens. The slab specimens are compacted using a roller compactor, which can create a smoother and more uniform surface. The ring specimens are created by combining multiple gyratory compacted samples, which may result in slight surface inconsistencies or gaps between the segments. Therefore, COF of ring-shaped specimens present slightly higher values. Surface irregularities are minimized through repeated polishing, and it tends to show no significant difference throughout polishing cycles.

It is noted that at the high speed of 80km/h the micro-texture decreases significantly and represents the pavement friction depending on macro-texture at the high speed. DFT measures the micro-texture of asphalt pavement. The friction number after 150,000 polishing cycles was chosen as the terminal skid-resistance level for evaluation. Therefore, the rest of the asphalt mixtures were compacted as ring-shaped specimens to test the frictional properties.

4.2.2 Deterioration analysis of laboratory asphalt mixture skid resistance

Table 4-6 summarizes the friction-based performance of laboratory asphalt mixtures. Figure 4-11 and Figure 4-12 illustrate the relationship between the decrease in COF and the chemical composition of asphalt mixtures, specifically silica dioxide (SiO₂) and iron dioxide (Fe₂O₃). The relative percentage decrease in COF (delta COF) is calculated as the difference between polishing stage 1 (stage 2) and stage 10, which are formulated by Equation (4-1) and Equation (4-2). COF₁ includes the influence of the asphalt binder film that is present on the aggregate surface at the start of testing. COF₂ was calculated after the asphalt binder film has worn off and COF₂ more accurately reflects the bare aggregate surface. Therefore, delta COF₂ represents the polishing resistance of the mineral material, free from the effects of asphalt. The percentage change makes deterioration relative to their starting performance, enabling fairer comparisons. The linear regression were employed to model and describe this relationship.

$$\text{Delta } COF_1 = \frac{COF_1 - COF_{10}}{COF_1} \times 100\% \quad (4-1)$$

$$\text{Delta } COF_2 = \frac{COF_2 - COF_{10}}{COF_2} \times 100\% \quad (4-2)$$

Table 4-6 Frictional-based performance results.

<i>TDOT No.</i>	<i>Initial COF</i>	<i>Terminal COF</i>	<i>Delta COF₁</i> (%)	<i>Delta COF₂</i> (%)	<i>SiO₂+Fe₂O₃</i> (%)	<i>Polish-resistant</i> (%)
1230674	0.59	0.53	10.17	8.62	62.66	95.5
1230715	0.58	0.50	13.79	18.03	58.22	97.5
2230203	0.61	0.39	36.07	25.00	28.16	79.5
2230259	0.61	0.40	34.43	28.57	36.83	81.25
2230260	0.56	0.36	35.71	33.33	19.80	84.25

3230061	0.50	0.38	24.00	28.30	44.36	82.5
4230043	0.54	0.39	27.78	11.36	74.86	79.25
4230095	0.51	0.39	21.57	17.02	72.98	75.5

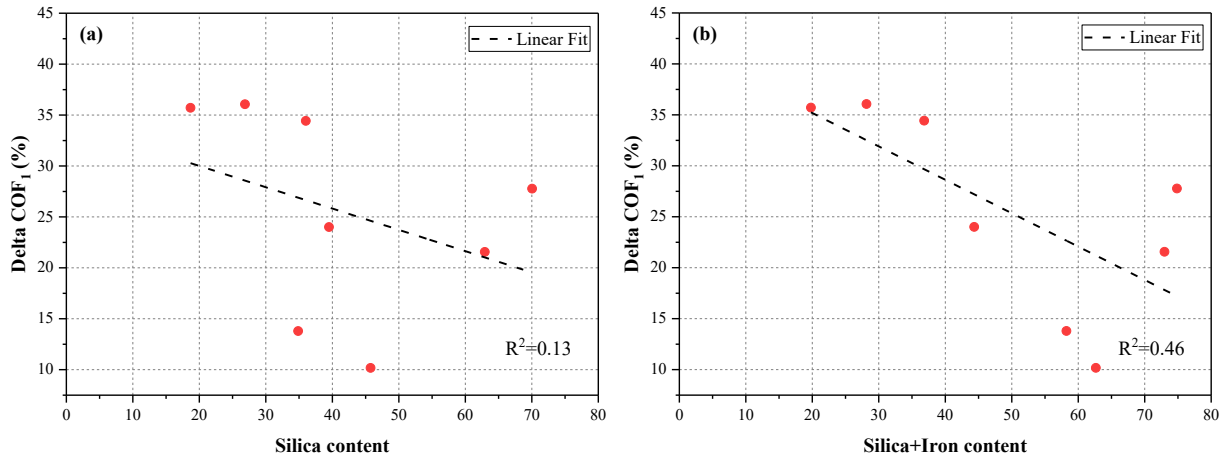


Figure 4-11 Correlation between decrease of COF₁ and chemical composition.

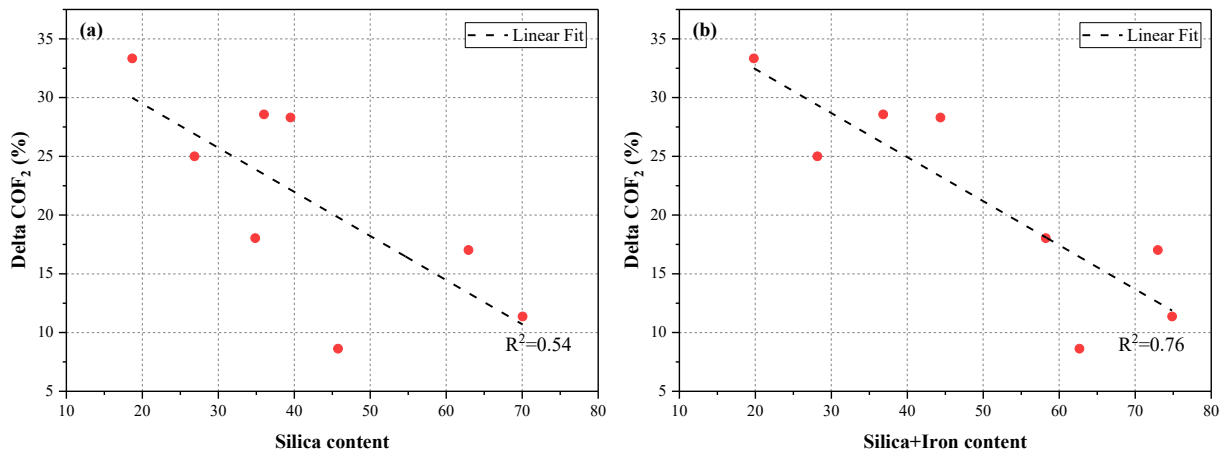


Figure 4-12 Correlation between decrease of COF₂ and chemical composition.

Figure 4-11(a) illustrates a weak negative correlation since silica content alone cannot explain much of the variation in initial polishing resistance when asphalt binder is present. Figure 4-11(b) proves slightly improved correlation when combining Iron into consideration. In Figure 4-12(a), $R^2 = 0.54$ indicates a moderate correlation between silica content and Delta COF₂. This suggests that once the asphalt binder is removed, the underlying relationship between aggregate mineralogy and polishing resistance becomes clearer. Silica-rich aggregates, known for their hardness and superior wear resistance, are better to retain surface texture, resulting in a lower percentage loss of friction. Figure 4-12 (b) further strengthens this finding, with a stronger correlation ($R^2 = 0.76$) observed between Delta COF₂ and the combined content of silica and iron. This implies that mineral composition, the presence of both silica and iron-rich, is highly predictive of long-term skid resistance after the asphalt coating has worn off. These results

support the conclusion that aggregates with higher percentage of polish-resistant minerals are more durable and better suited for maintaining pavement friction over time.

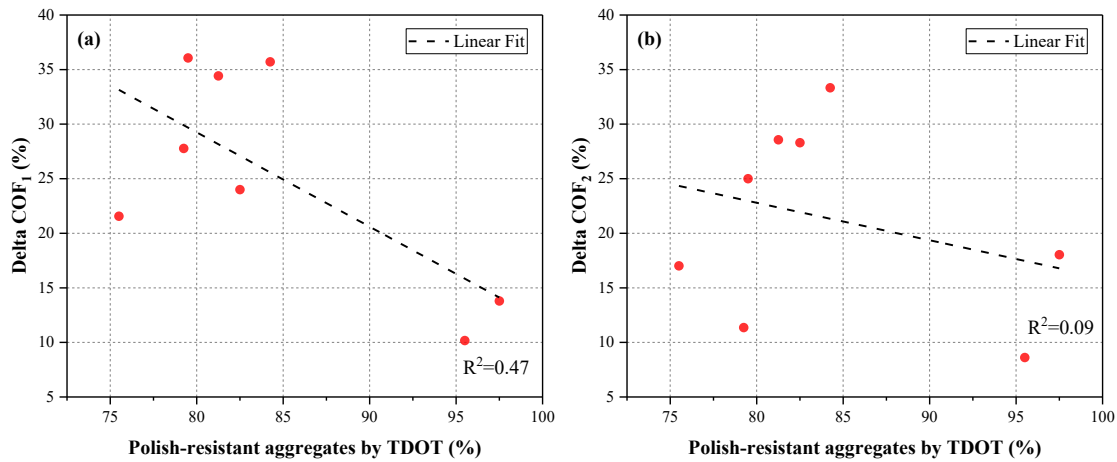


Figure 4-13 Correlation between decrease of COF and polish-resistant percentage.

As shown in Figure 4-13, the correlation between Delta COF and TDOT's polish-resistant aggregate percentage is relatively weak. This limitation is likely from the inclusion of natural sand in TDOT's classification as a polish-resistant aggregate. Natural sands, often used as fine aggregates, tend to be stripped away by traffic quickly, which can potentially result in weak correlation.

In Figure 4-14, the terminal COF, an indicator of long-term frictional performance, is more strongly correlated with the TDOT-defined polish-resistant aggregate percentage ($R^2 = 0.76$) than with the measured silica + iron content ($R^2 = 0.16$). This indicates that TDOT's classification of polish-resistant aggregates, which considers multiple mineral and performance criteria, is a better predictor of terminal COF. The trend suggests that higher polish-resistant aggregate content results in higher terminal COF values.

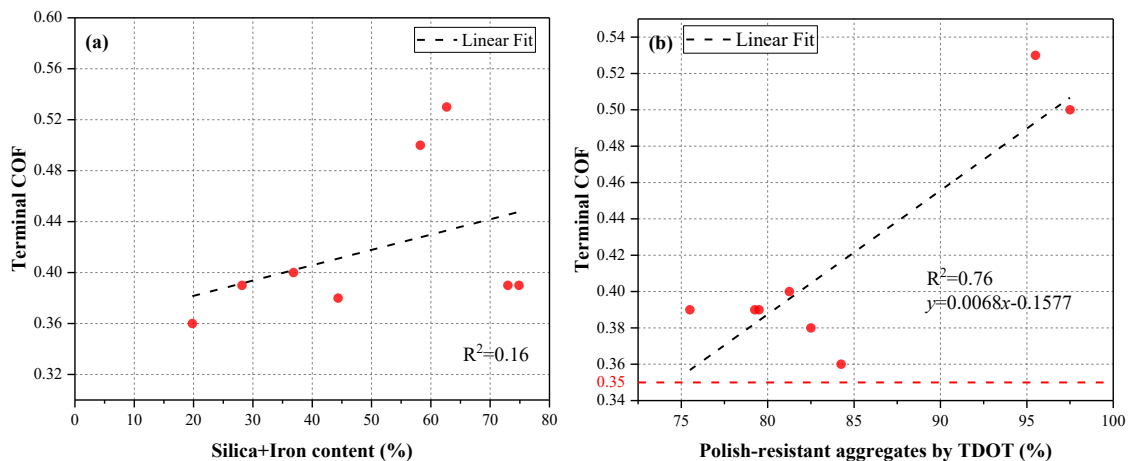


Figure 4-14 Correlation between terminal COF and polish-resistant materials.

The reduction in COF and the terminal COF reflect two different aspects of pavement surface performance. COF reduction represents the magnitude of friction loss over time, typically from

early life to a more stabilized stage. It captures how quickly the surface deteriorates under polishing effects or material loss. In contrast, terminal COF refers to the long-term residual friction value that remains after extended traffic exposure, serving as a measure of long-term skid resistance. TDOT's definition of polish-resistant aggregates shows a strong correlation with terminal COF. It is likely because it includes hard, durable materials that retain friction over time. However, its correlation with COF reduction is weaker, partly due to the inclusion of natural sand.

Therefore, both of those variables are combined to determine the most accurate model for the prediction of terminal COF. Table 4-7 presents a comparison of different variable combinations to model the terminal COF. R^2 and root mean square error ($RMSE$) are evaluation metrics. From Table 4-7, combining both mineral content and polish-resistant content (%) further enhances the model's accuracy, achieving an R^2 of 0.88 and $RMSE$ of 0.0203.

Table 4-7 Terminal COF Prediction performance of regression models.

<i>Variables</i>	R^2	$RMSE$
<i>Silica-Iron Mineral Content (%)</i>	0.16	0.0530
<i>Polish-resistant Content (%)</i>	0.76	0.0283
<i>Mineral Content + Polish-resistant Content Combined (%)</i>	0.88	0.0203

Therefore, the terminal COF is formulated by Equation (4-3):

$$\text{Terminal COF} = -0.193 + 0.0010X_1 + 0.0066X_2 \quad (4-3)$$

where X_1 is the silica-iron mineral content (%), X_2 is the polish-resistant aggregate content (%).

The regression analysis highlights the significant role of silica-iron mineral content in determining terminal COF, especially when the polish-resistant content is a constant. The multivariate regression model explains 88% of the variation in terminal COF. According to the regression equation (4-3), if the polish-resistant aggregate content remains at 75%, a minimum of 50% silica-iron content is required to achieve a terminal COF greater than 0.35. This underscores the importance of not relying on polish-resistant content alone but ensuring a sufficient level of silica-iron mineral composition to maintain long-term skid resistance.

4.3 Field skid resistance measurement

In addition to the laboratory observation, a comprehensive statistical analysis was performed with the collected field test data. DFT20 and DFT60 from the field segments are presented in Figure 4-15. The DFT20 is paired with the MPD to calculate the IFI, which provides a comprehensive evaluation of pavement frictional performance. Additionally, the DFT60 is used to compare its results with the SN40 obtained from the locked-wheel skid trailer, ensuring consistency and validation across different friction assessment methods. In Figure 4-15, the left y axis shows the values for DFT20, DFT60, and IFI, which provide an indication of pavement surface friction. The right y axis represents the macrotexture of the pavement surface, showing the mean profile depth (MPD) values.

DFT60 and DFT20 generally follow similar trends. Measurements on the left-wheel, right-wheel, and pavement shoulder are included in Figure 4-15 and it shows fluctuation on the same segments. The greater values were measured from the pavement shoulder. IFI stays consistently lower than the DFT and MPD values. The MPD values exhibit significant fluctuations, indicating variability in pavement macrotexture across different segments. Peaks in MPD suggest rougher macro-textures, which generally contribute to better friction but may also introduce surface irregularities. Segment 9 is the OGFC surface layer and presents higher MPD accordingly. Figure 4-15 indicate that there is no significant difference between DFT60 and DFT20. DFT20, DFT60, and IFI present similar trends over test segments.

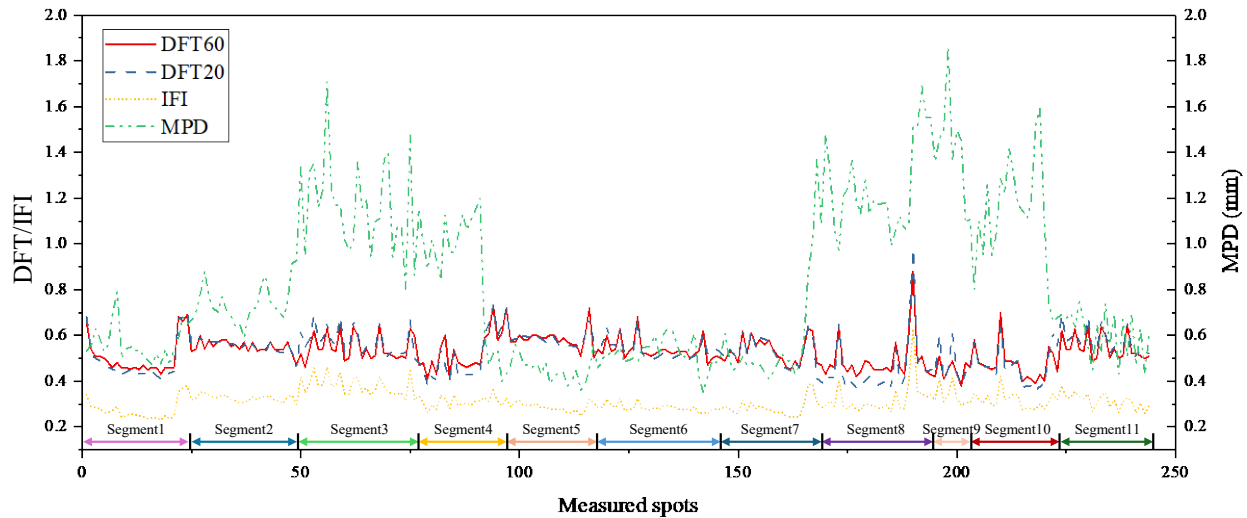


Figure 4-15 DFT and IFI from collected data.

To further investigate the interaction between friction and texture, the linear regression model was used to assess the correlation between those indicators, as shown in Figure 4-16, Figure 4-17, and Figure 4-18, respectively.

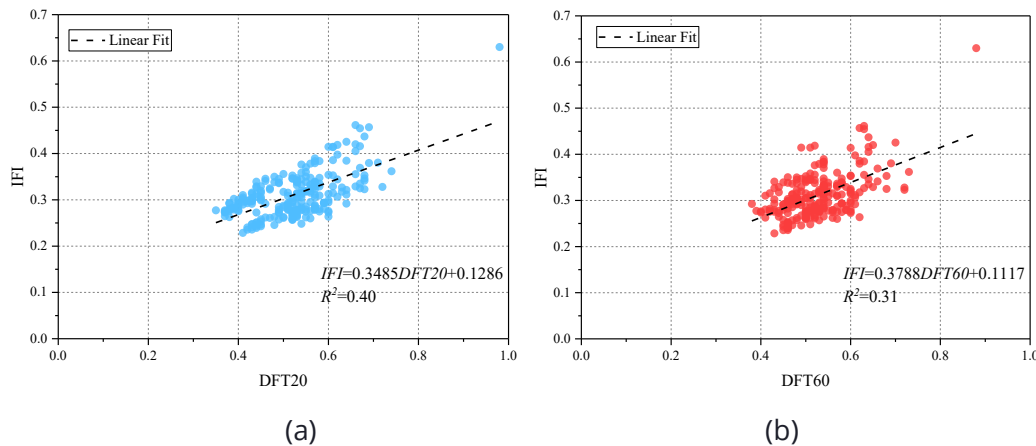


Figure 4-16 (a) Correlation between IFI and DFT60; (b) Correlation between IFI and DFT20.

It is noted that the simple linear regression model could explain 40% variation for IFI with DFT20 since IFI is calculated by a nonlinear model in Figure 4-16. With the increase in DFT values, the IFI shows an increasing trend. DFT20 provides a higher R^2 compared to DFT60, likely because lower-

speed friction values capture surface micro-texture more effectively. However, the relatively low R^2 values indicate that macro-texture (MPD) and other surface characteristics must be considered for a comprehensive evaluation of pavement friction.

The relationship between macro-texture and micro-texture is analyzed in Figure 4-17. The figure demonstrates that there is no significant linear correlation between MPD and COF, as indicated by the low R^2 value of 0.08. This finding is consistent with previous studies [20] and aligns with expectations, given that the DFT primarily measures micro-texture, while MPD serves as an indicator of macro-texture. Consequently, the IFI is employed to provide a comprehensive evaluation of pavement skid resistance by incorporating both macro- and micro-texture characteristics.

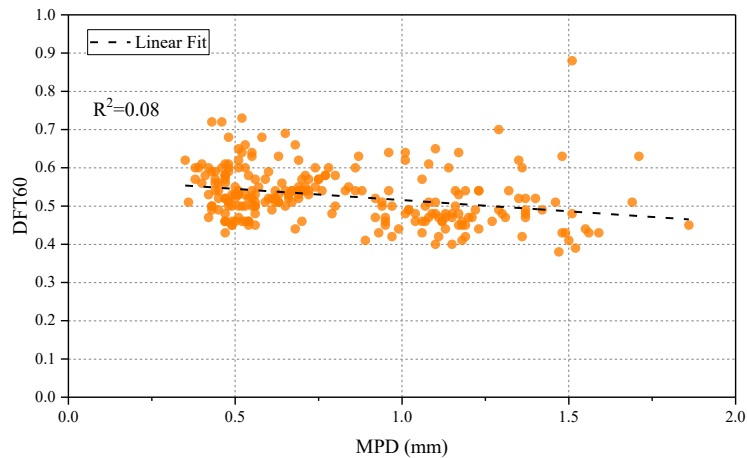


Figure 4-17 Correlation between MPD and COF at 60km/h (DFT60).

In addition to the correlation between friction and texture, Figure 4-18 presents the relationship between two profile-based indicators, MPD and MTD. The R^2 for this correlation is 0.8997, indicating a strong linear relationship between the two parameters. This high correlation suggests that MPD and MTD measurements can be used interchangeably with a high level of confidence, making them reliable alternatives for texture evaluation.

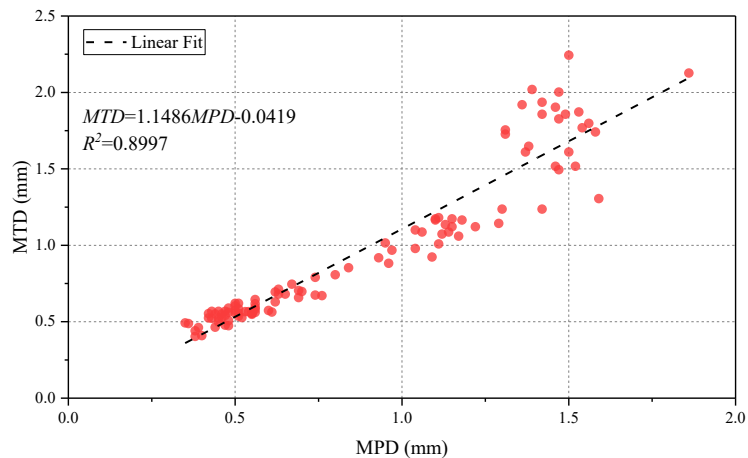


Figure 4-18 Correlation between MPD and MTD.

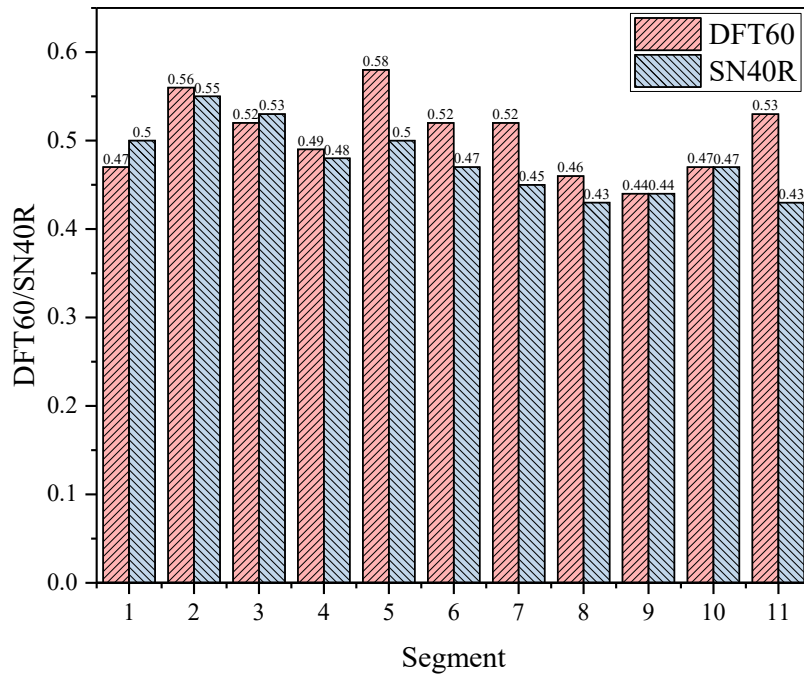


Figure 4-19 Field friction measurements by DFT and LWST.

As shown in Figure 4-19, this bar chart presents the average friction measurement results across 11 pavement segments using two different methods: the DFT represented by COF, and the LWST represented by SN40R. In most segments, the COF values are higher than the SN40R values. DFT measures friction on a circular path, which captures both polished and unpolished areas of the pavement, potentially leading to higher average values. LWST measures friction directly on the wheel path, where surface polishing due to traffic is more pronounced, resulting in lower average values compared to COF.

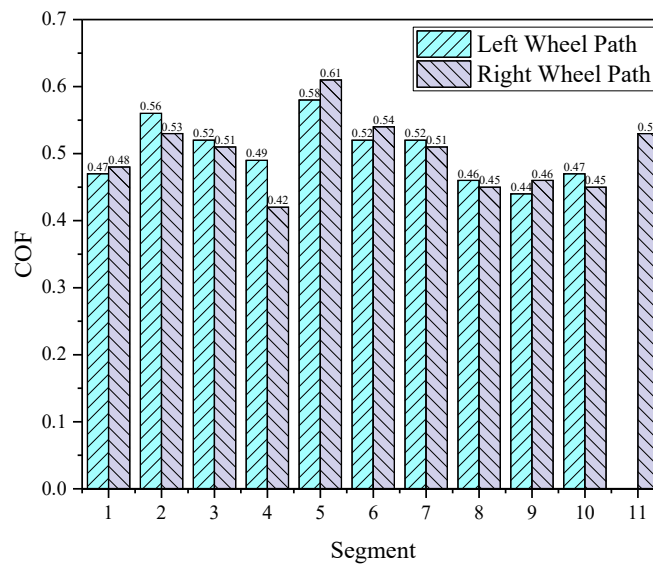


Figure 4-20 COF measured by DFT on different wheel paths.

Figure 4-20 presents the COF measured using the DFT on both the left and right wheel paths across 11 pavement segments. The left wheel path was not measured for segment 11 due to high traffic volume, which made it unsafe to conduct measurements in that lane. Since the p-value (0.448) of paired t-test is significantly greater than 0.05, this confirms that there is no statistically significant difference between the COF values measured on the left and right wheel paths. In most segments, the COF values for the left and right wheel paths are within close range, indicating similar frictional properties across both paths.

Table 4-8 summarizes the field test segments with material information, service years and AADT to make comparisons.

Table 4-8 Summary of the field test segments.

<i>Segment</i>	<i>Mixture type</i>	<i>Aggregates</i>	<i>Polish-resistant materials (%)</i>	<i>Service years</i>	<i>AADT</i>
1	411-D (PG 70-22)	20% Gravel + 25% Granite + 25% Natural Sand + 19% soft limestone + 10%RAP + 1% filler	77.5	2	30,658
2	411-D (PG 76-22)	35% Gravel + 20%Slag + 10%soft limestone + 25% Natural Sand + 10% RAP	87.5	4	11,013
3	411-TLD (PG 64-22)	50% Gravel + 25% Natural Sand + 15% soft limestone + 10% RAP	82.5	2.5	12,445
4	411-TLD (PG 64-22/67-22)	50% Gravel + 25% Natural Sand + 15% soft limestone + 10% RAP	82.5	3	4,562
5	411-TLD (PG 70-22)	50% Gravel + 25% Natural Sand + 15% soft limestone + 10% RAP	82.5	3	7,507
6	411-TL (PG 64-22)	73% Granite + 10% Granite + 15% RAP + 15% RAP	94.25	11	1,350
7	411-D (PG 70-22)	45% type IV hard limestone + 22% soft limestone + 23% Natural Sand + 10% RAP	75.5	2	2,019
8	411-D (PG 70-22)	40% type II hard limestone + 21% soft limestone + 24% Natural Sand + 15%RAP	75.25	2	5,441

9	411-OGFC (PG 76-22)	75% type II hard limestone + 25% soft limestone	75	2	18,188
10	411-D (PG 70-22)	48% Gravel+ 20% soft limestone + 22% Natural Sand + 10%RAP	77.5	4	10,536
11	411-D (PG 76-22)	47% Gravel + 17% soft limestone + 21% Natural Sand + 15%RAP	79.25	2	69,131

Figure 4-21 shows the collection of field cores from the left wheel path. Figure 4-22 presents the silica content distribution across the 11 segments. Field cores were collected, and aggregates were extracted from three cores for each segment. Aggregates retained on the No. 4 sieve were analyzed for silica content using XRF. The primary aggregates retained on the No. 4 sieve for segments 7, 8, and 9 are Type IV, Type II, and Type II limestone, respectively. Among these, segment 7, composed of Type IV limestone, exhibits the lowest silica content.

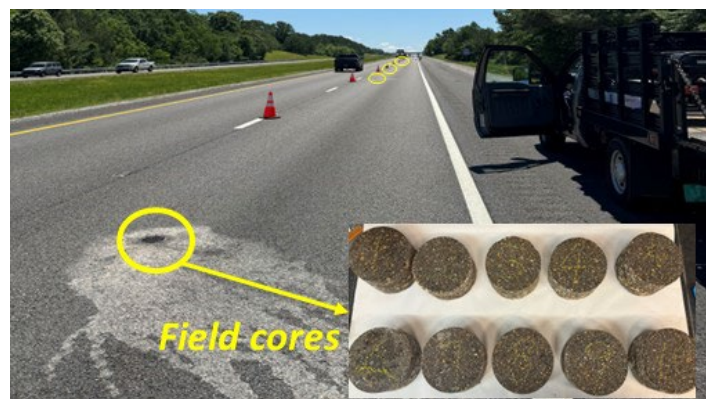


Figure 4-21 Collected field cores for the analysis of chemical composition.

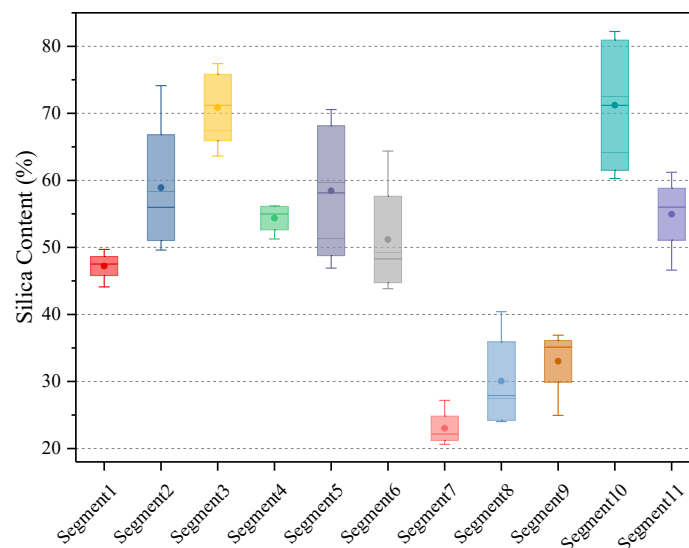


Figure 4-22 Silica content distribution over 11 segments.

To examine the impact of silica content on friction deterioration, Figure 4-23 visualizes the decrease in COF (Delta COF) expressed in equation (4-4) in relation to AADT, service year, and silica content. Since segment S9 features an OGFC pavement surface, which is not directly comparable to dense-graded pavement surfaces, Figure 4-23 focuses on 10 dense-graded segments to analyze the deterioration of pavement skid resistance. In Figure 4-23, S1 corresponds to segment 1, with similar notations applied to the other segments. The x-axis represents the service year, while the left y-axis shows the decrease in COF (Delta COF). The color bar on the right side of the plot indicates the silica content (%) of the data points, with a gradient ranging from dark purple (low silica content) to yellow (high silica content).

$$\Delta COF = |COF_{initial} - COF_t| \quad (4-4)$$

where $COF_{initial}$ represents the initial pavement friction number, and it is represented by the measurement on the pavement shoulder. COF_t means the pavement friction coefficient at the specific service year.

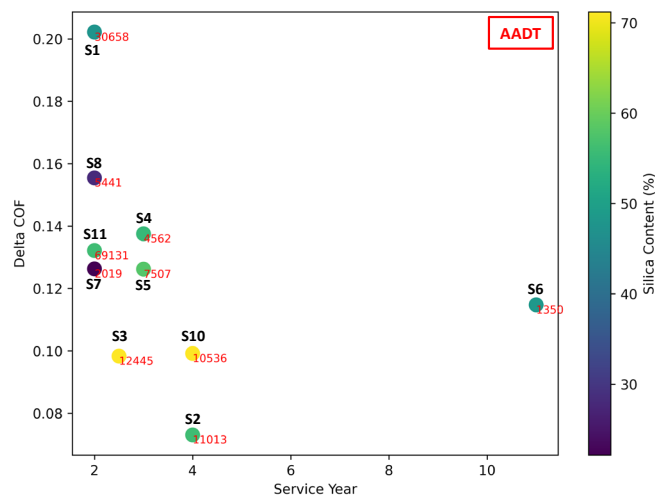


Figure 4-23 Decrease in COF compared with service year, AADT, and silica content.

For pavements with 2 to 3 years of service, higher silica content is associated with greater skid resistance, even under higher traffic loads. The following comparison evaluates segments by comprehensively considering factors such as AADT, service life, and silica content:

- S11 shows smaller changes in COF compared to S1, despite having nearly half the AADT of S1, likely due to S11's 10% higher silica content.
- When comparing sites like S7 and S8 with similar silica content, higher AADT results in more significant COF deterioration.
- This trend is also evident in S3 and S10, where the same degradation level is reached over a prolonged service period with reduced traffic exposure.
- However, S2, which has lower silica content and higher AADT, exhibits less COF reduction compared to S10. The primary coarse aggregates used in S2 are gravel and slag, while S10 primarily uses gravel. While slag does not increase silica content, it contributes to improved skid resistance due to the iron oxide, explaining S2's lower COF reduction. Results demonstrate that slag aggregates have superior hardness and wear resistance.

Chapter 5 Conclusion

The skid resistance of asphalt mixtures is characterized by micro- and macro-textures. The micro-texture is associated with the polishing properties of aggregates at the mixture surface. The macro-texture is related to gradation, density, shape, angularity, and arrangement of aggregates within the mixture layer. Frictional properties of aggregates and RAP are quantitatively evaluated by the silica content. The micro-texture frictional properties of aggregates and RAP have been evaluated by XRF, BPN, Micro-Deval, AIMS. In addition, TWPD was utilized to simulate the traffic polishing effort to investigate the long-term frictional deterioration of asphalt mixtures. DFT and CTM were deployed to measure the skid resistance-related indicators along the circular polishing track. The field pavement skid resistance tests were conducted to correlate the relationship between DFT and LWST.

The conclusions are drawn as follows:

- The DFT proves to be a practical tool for friction assessment with both laboratory and field applications. Its integration with laboratory accelerated polishing tests supports the development of friction performance-based mixture designs.
- There is no significant difference between the slab and ring-shaped specimens for COF and texture parameters, measured by DFT and CTM. The ring-shaped specimen could be used as an alternative method to evaluate the skid resistance in the laboratory.
- DFT measures friction on a circular path, which captures both polished wheel path and unpolished areas of the pavement in the field, potentially leading to higher average values. LWST measures friction directly on the wheel path, resulting in lower average values compared to COF.
- The uniformity of aggregates is crucial for accurately determining SiO_2 contents using XRF. Since XRF measures the surface-level elemental composition, variations in particle uniformity can significantly impact the precision and reliability of the measurements. It is recommended to use aggregates passing 3/8 in. (9.5mm) and retained on No.4 (4.75mm) sieves for SiO_2 content measurement for both aggregates and RAP, ensuring a more reliable test result.
- The SiO_2 of RAP treated either by TCE or hammer can be efficiently measured by XRF. Laboratory-produced RAP demonstrated that the SiO_2 content was close to the virgin aggregates when washed by TCE three times or crushed by a hammer. However, when tested with field-sampled RAP, the SiO_2 content of TCE-treated RAP is found to have a lower standard deviation compared to those treated by a hammer. It is recommended that TCE could produce more accurate results for both laboratory-produced and field-sampled RAP.
- Correlation between the SiO_2 content and frictional properties of aggregates and RAP has been established. SiO_2 content has shown significant correlations with PSV, and texture loss, with R^2 Values of 0.81, and 0.78 respectively. With the increase of SiO_2 contents, PSV also increases while relative texture loss decreases.
- The COF values for the left and right wheel paths are generally comparable across all segments, with no significant differences observed. In most segments, the COF values for

the left and right wheel paths are within close range, indicating similar frictional properties across both paths.

- It is suggested that the combination of silica and iron content ($\text{SiO}_2+\text{Fe}_2\text{O}_3$) provides a more accurate prediction of changes in COF. Asphalt mixture with slag shows a significantly lower Delta COF, further supporting the role of slag in improving skid resistance due to its rich iron content.
- The multiple linear regression model, which incorporates both silica-iron mineral content and polish-resistant aggregate percentage, explaining 88% of the variation in terminal COF. The result indicates that the model provides a reliable representation to determine the terminal COF.
- According to the regression analysis, if the polish-resistant aggregate content remains at 75%, a minimum of 50% silica-iron content is required to achieve a terminal COF (measured by DFT) greater than 0.35 based on laboratory findings. This underscores the importance of not relying on polish-resistant content alone but ensuring a sufficient level of silica-iron mineral composition to maintain long-term skid resistance.

References

1. S. Kouchaki, H. Roshani, J. A. Prozzi, N. Z. Garcia, J. B. Hernandez, Field investigation of relationship between pavement surface texture and friction[J]. *Transportation Research Record*. **2672**(40)(2018): p. 395-407.
2. F. Guo, J. Pei, J. Zhang, R. Li, B. Zhou, Z. Chen, Study on the skid resistance of asphalt pavement: A state-of-the-art review and future prospective[J]. *Construction and Building Materials*. **303**(2021): p. 124411.
3. M. Yu, Z. You, G. Wu, L. Kong, C. Liu, J. Gao, Measurement and modeling of skid resistance of asphalt pavement: A review[J]. *Construction and building materials*. **260**(2020): p. 119878.
4. Y. Hu, Z. Sun, Y. Han, W. Li, L. Pei, Evaluate pavement skid resistance performance based on Bayesian-LightGBM using 3D surface macrotexture data[J]. *Materials*. **15**(15)(2022): p. 5275.
5. S. Chen, X. Liu, H. Luo, J. Yu, F. Chen, Y. Zhang, T. Ma, X. Huang, A state-of-the-art review of asphalt pavement surface texture and its measurement techniques[J]. *Journal of Road Engineering*. **2**(2)(2022): p. 156-180.
6. F. Guo, J. Zhang, Z. Chen, M. Zhang, J. Pei, R. Li, Investigation of friction behavior between tire and pavement by molecular dynamics simulations[J]. *Construction and Building Materials*. **300**(2021): p. 124037.
7. X. Zhu, Y. Yang, H. Zhao, D. Jelagin, F. Chen, F. A. Gilabert, A. Guarin, Effects of surface texture deterioration and wet surface conditions on asphalt runway skid resistance[J]. *Tribology International*. **153**(2021): p. 106589.
8. M. Pomoni, C. Plati, Skid resistance performance of asphalt mixtures containing recycled pavement materials under simulated weather conditions[J]. *Recycling*. **7**(4)(2022): p. 47.
9. J. Hall, K. L. Smith, L. Titus-Glover, J. C. Wambold, T. J. Yager, Z. Rado, Guide for pavement friction[J]. Final Report for NCHRP Project. **12**(09): p. 43.
10. J. Zhong, J. Zhang, K. Huang, P. Blankenship, Y. Ma, R. Xiao, B. Huang, An investigation of texture-friction relationship with laboratory ring-shaped asphalt mixture specimens via close-range photogrammetry[J]. *Construction and Building Materials*. **442**(2024): p. 137508.
11. ASTM, Standard test methods for chemical analysis of limestone, quicklime, and hydrated lime[J]. (2011).
12. A. ASTM, Standard test method for measuring surface frictional properties using the British pendulum tester[J]. ASTM International West Conshohocken, PA, (2013).
13. E. ASTM. *Standard test method for measuring surface frictional properties using the dynamic friction tester*. 1911. ASTM.
14. A. S. f. Testing Materials, *Standard test method for skid resistance of paved surfaces using a full-scale tire*. 1998, ASTM International West Conshohocken, PA, USA.
15. A. Standard, E670-09, 2009[J]. Standard Test Method for Testing Side Force Friction on Paved Surfaces Using the Mu-Meter. ASTM International, West Conshohocken, PA, (2008).
16. E. ASTM, Standard Test Method for Friction Coefficient Measurements between Tire and Pavement Using a Variable Slip Technique[J]. (2006).
17. ASTM, Standard test method for measuring pavement macrotexture depth using a volumetric technique[J]. Designation: E 965-96, (2006).
18. E. ASTM, 2380; Standard Test Method for Measuring Pavement Texture Drainage Using an Outflow Meter[J]. ASTM International: West Conshohocken, PA, USA, (2010).
19. ASTM, Standard test method for measuring pavement macrotexture properties using the circular track meter[J]. E2157-09, (2009).

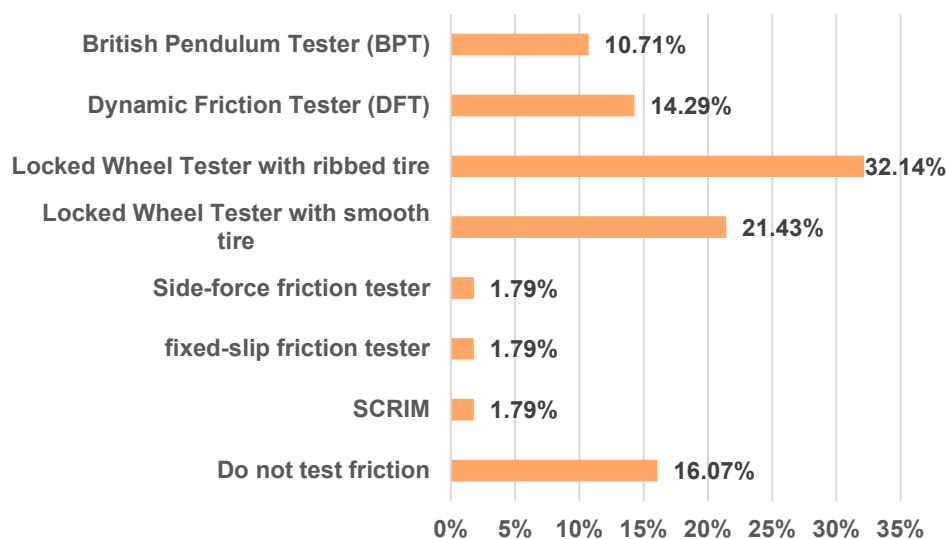
20. T. M. Al Rousan, *Characterization of aggregate shape properties using a computer automated system*. 2004: Texas A&M University.
21. I. Mohi Ud Din, M. S. Mir, Effect of copper slag and reclaimed asphalt pavement on the skid resistance of asphalt mixes[J]. *International Journal of Pavement Engineering*. **23**(11)(2022): p. 3983-3996.
22. S. Hu, F. Zhou, T. Scullion, E. Fernando, M. I. Souliman, Quantifying the impact of reclaimed asphalt pavement on the skid resistance of surface mixtures[J]. *Transportation research record*. **2677**(11)(2023): p. 615-628.
23. J. Zhong, Y. Ma, G. Cheng, R. Xiao, U. Martinez, B. Huang, Quantitative Evaluation of Microtexture Frictional Properties of Aggregates and Reclaimed Asphalt Pavement[J]. *Journal of Materials in Civil Engineering*. **36**(12)(2024): p. 04024421.
24. R. S. McDaniel, A. Shah, K. J. Kowalski, Development of a friction performance test for compacted asphalt mixtures[J]. (2018).
25. M. Heitzman, F. Gu, A. Welderufael, *Three wheel polishing device and dynamic friction tester accelerated laboratory friction testing repeatability and reproducibility study*. 2019.
26. R. Rasmussen, R. Sohaney, P. Wiegand, D. J. T. B. Harrington, Measuring and Analyzing Pavement Texture: Concrete Pavement Surface Characteristics Program[J]. (2011).
27. A. E-15, *Standard practice for calculating pavement macrotexture mean profile depth*. 2015, ASTM International West Conshohocken, PA.
28. W. Goodwin, A. Moore, *Tennessee's inventory of pavement skid resistance, in Skid Resistance of Highway Pavements*. 1973, ASTM International.
29. C. Allen, T. Peterson, *Using pavement texture to screen and target annual skid number assessment*. 2019, Parametrix.
30. T. S. Arnold, *How to Determine the Silica Content of Limestone Aggregates at the Quarry in 20 Minutes with No Sample Preparation*. 2020.
31. S. Hu, F. Zhou, T. Scullion, E. Fernando, M. Souliman, *Develop Surface Aggregate Classification of Reclaimed Asphalt Pavement: Technical Report*. 2022, Texas A&M Transportation Institute.

Appendices

Through an online survey of the State and Provincial Departments of Transportation (DOTs). The survey was sent to 50 states in the US and 33 responses were received. This summary is based on the responses of the following states: Wyoming (WY), Colorado (CO), Kentucky (KY), Maine (ME), Utah (UT), Vermont (VT), New York (NY), South Dakota (SD), South Carolina (SC), Florida (FL), Washington (WA), Nebraska (NE), California (CA), Georgia (GA), Delaware (DE), Texas (TX), Mississippi (MS), Alabama (AL), Arkansas (AR), Illinois (IL), North Carolina (NC), Alaska (AK), Hawaii (HI), Ohio (OH), Massachusetts (MA), Minnesota (MN), Nevada (NV), Kansas (KS), Connecticut (CT), Oregon (OR), West Virginia (WV), Indiana (IN), North Dakota (ND).

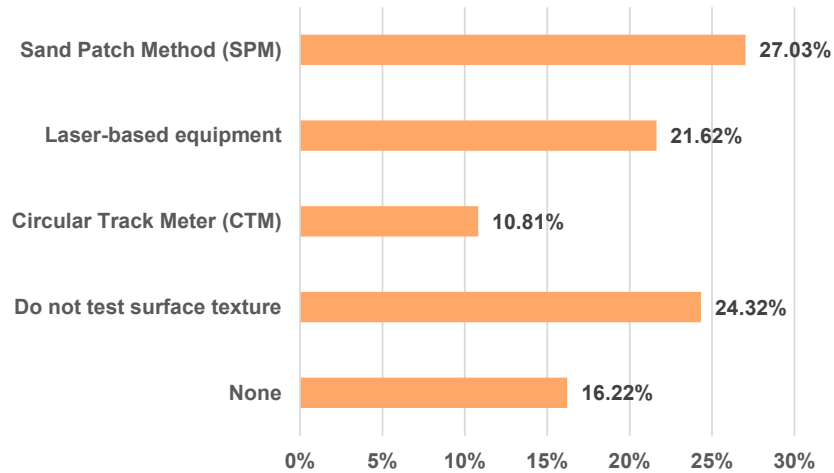
This questionnaire is prepared by the University of Tennessee, aiming to increase the use of local materials with low silica content to achieve a more economical asphalt-wearing surface. According to the responses, 21.1% of states do not conduct pavement friction tests. For most states performing friction tests, friction number is used for pavement skid resistance evaluation. The friction test frequency for interstate and state routes is very low, fewer states perform quarterly or yearly friction tests. 63.6% of states did not consider the season influencing when testing in different seasons. Limestone is a commonly used aggregate while 84.8% states do not have a minimal silica content to control pavement skid resistance. 81.8% of states do not test RAP frictional properties when using RAP for construction. 51.5% of states choose proper materials to provide adequate pavement friction performance. The following are the details of the survey:

(1) What is the equipment used for pavement friction coefficient measurement in your state?



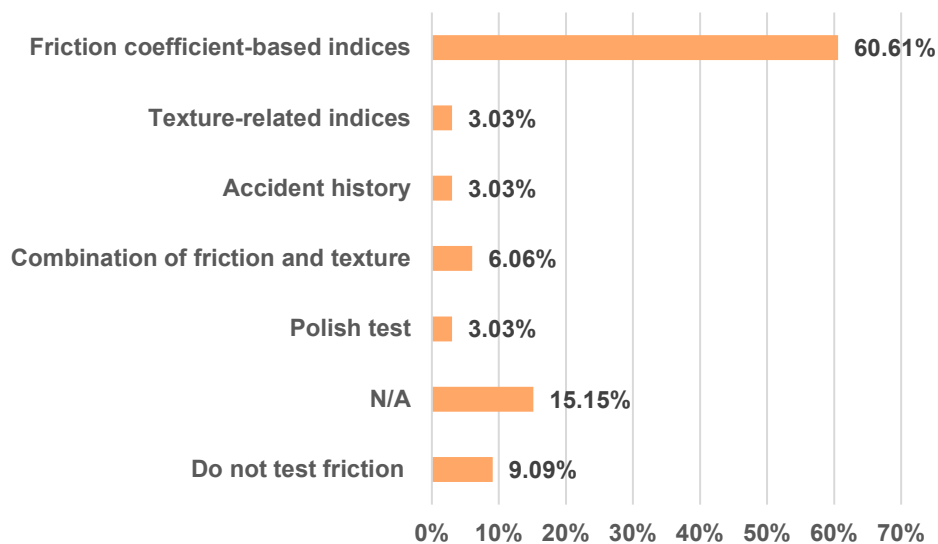
Note: Locked-wheel testers are frequently used for pavement friction coefficient measurement. Ribbed and smooth tire are sensitive to micro- and macro-texture to contribute to pavement skid resistance. DFT accounts for 14.29% for friction tests. In addition, 16.07% of states do not test pavement friction.

(2) What is the equipment used for surface texture testing?



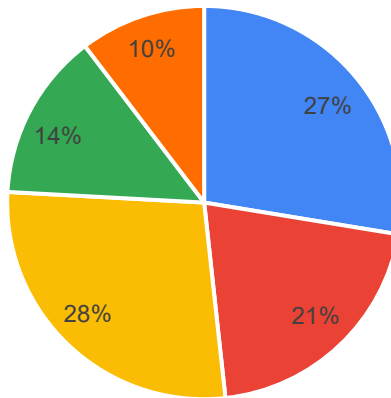
Note: SPM and Laser-based methods have been widely used for pavement texture testing. 24.32% of states do not measure pavement texture.

(3) How do you assess pavement friction performance?



Note: Friction coefficient-based indices like Skid Number (SN) or Friction Number (FN) are widely used to evaluate pavement friction performance. In addition, accident history is used for assessment.

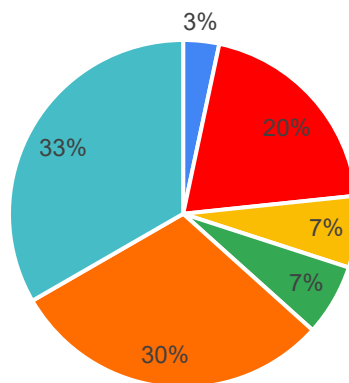
(4) The friction test frequency of interstate routes in your state?



■ Every year ■ Every two years ■ As needed ■ Do not test ■ N/A

Note: Usually, pavement friction measurement is not a monitoring task for most states. However, more than a quarter of states still consider pavement friction as a major concern for interstate routes and will perform friction test every year. 28% of states will measure pavement friction as needed.

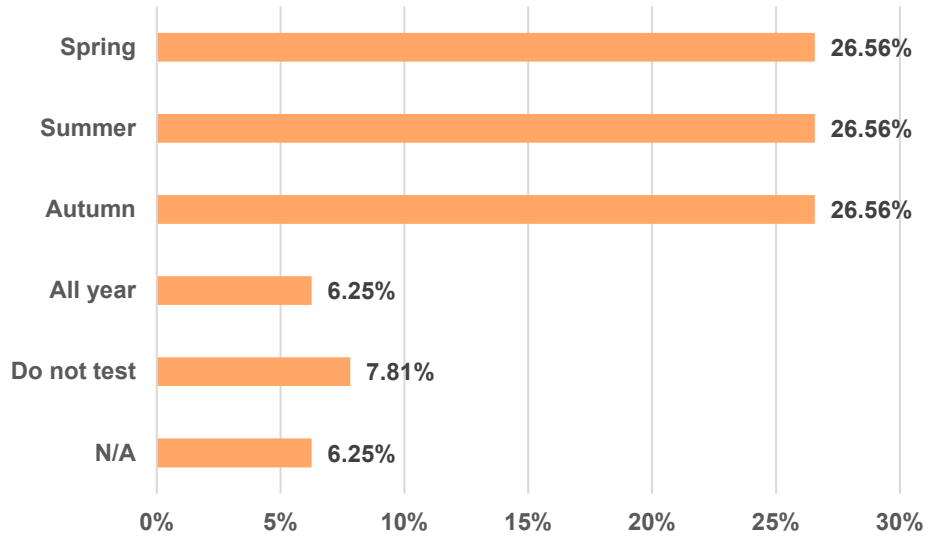
(5) The friction test frequency of state routes in your state?



■ Every year ■ Every two years ■ Every three years
 ■ Every four years ■ As needed ■ Do not test

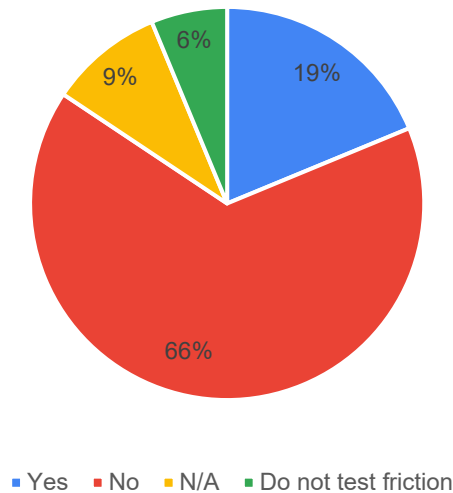
Note: Compared with interstate routes, only 3% of state routes will conduct pavement friction tests every year. 33% of states do not test friction for state routes and 30% of states will measure pavement friction as needed.

(6) During which seasons is pavement friction testing conducted?



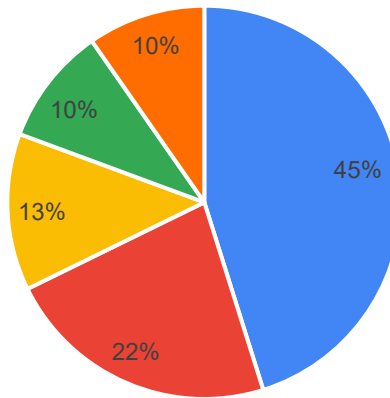
Note: Some states do not test pavement friction. Most states test friction from spring to autumn. 6.25% of states will test pavement friction in winter.

(7) Have you considered season influencing pavement surface friction (e.g., Use Correction factor)?



Note: 66% of states have not considered season influencing for pavement friction test. 19% of states will consider season effects to pavement surface friction for calibration.

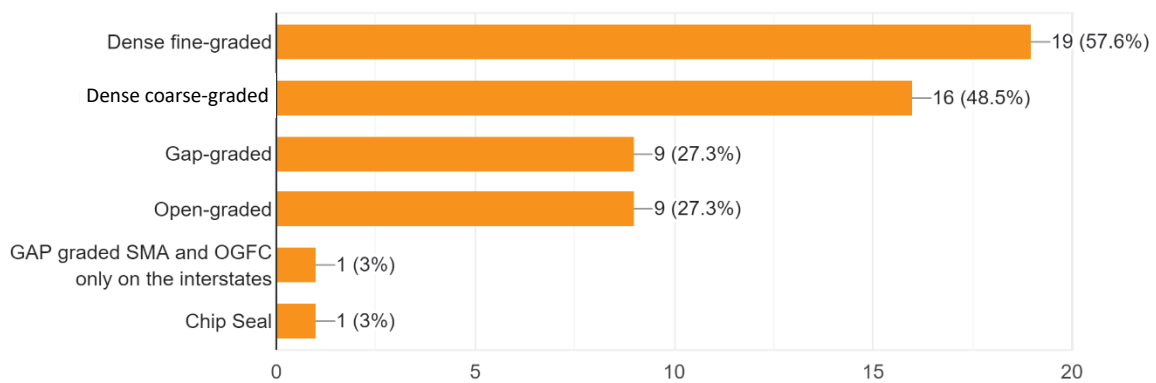
(8) Will friction testing be conducted on pavement distress section where there are cracks, potholes, or other distress?



■ Yes ■ No ■ N/A ■ Do not test friction ■ Depends on level of severity

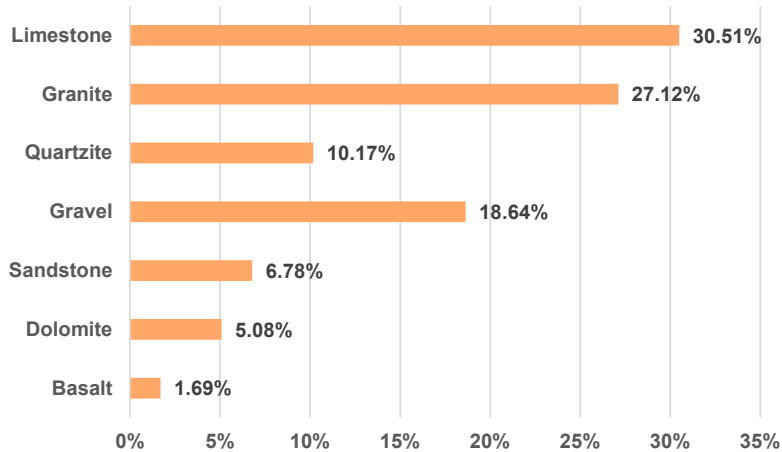
Note: 10% states rely on pavement distress severity level to decide whether they should test pavement friction on pavement distress section. 45% of states will test pavement friction on distress section.

(9) What is the commonly used surface asphalt mixture gradation in your state?



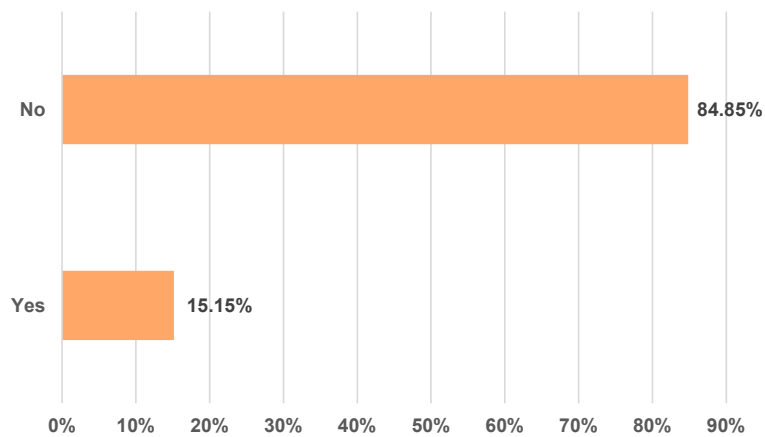
Note: Dense fine-graded asphalt mixture is widely used for pavement surface construction. 9% of states chose open-graded asphalt mixture to provide sufficient pavement skid resistance.

(10) What is the commonly used coarse aggregate type of surface mixtures in your state?



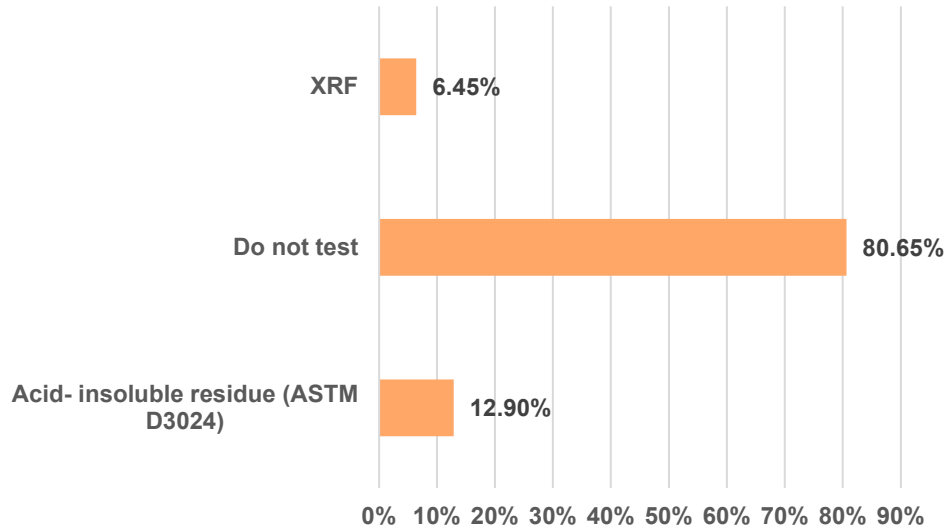
Note: Limestone is the widely used pavement construction aggregate. Some states choose limestone by silica content and non-carbonate content to improve pavement skid resistance.

(11) Do you have a minimal silica content in aggregate to guarantee pavement friction? (if yes, please specify your minimal silica content in other option)



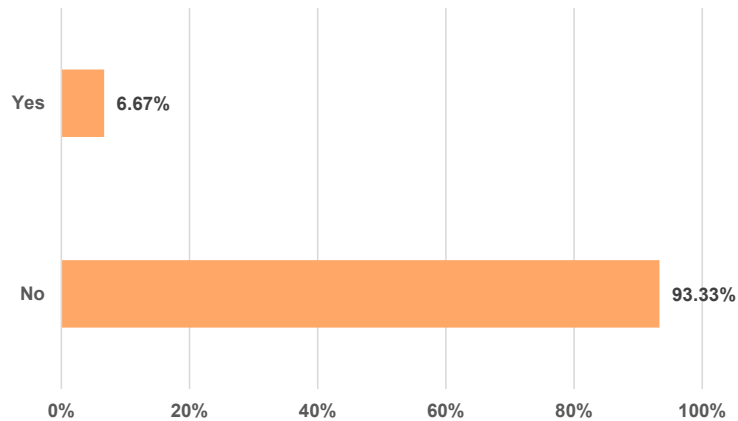
Note: 84.85% of states do not set the minimal silica content for surface aggregates. 15.15% of states have the minimal silica content of 10% in aggregates. In addition, they use blended aggregates to improve the content of non-skid materials.

(12) What is the method to test silica content?



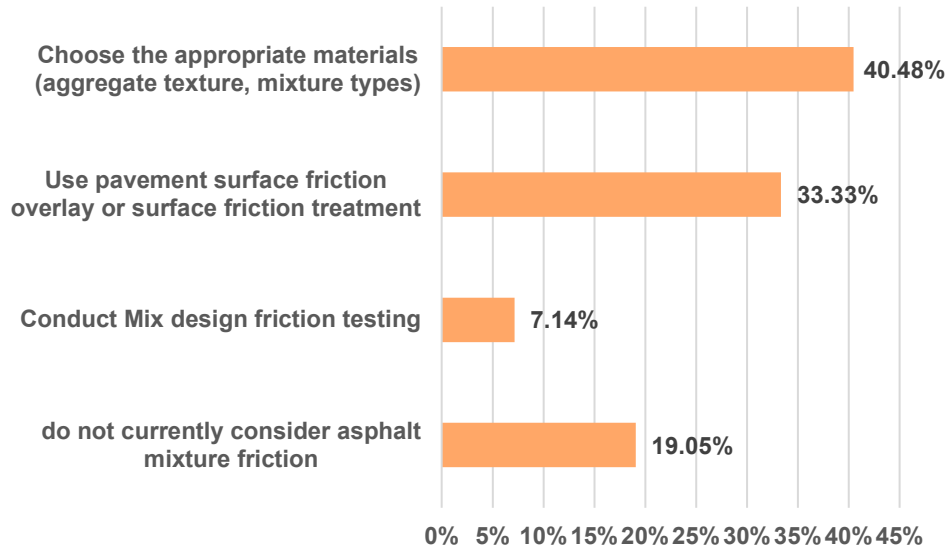
Note: most states do not control the silica content of aggregates and do not test silica content either. 6.45% of states use XRF to test silica content and 12.90% use acid-insoluble residue to make sure pavement anti-polishing performance.

(13) Do you control material frictional properties when using Reclaimed Asphalt Pavement (RAP)?



Note: It is noted that 93.33% states do not control the frictional properties of RAP. The pavement skid-resistance should be monitored for safety.

(14) How do you consider asphalt mixture friction?



Note: 40.48% of states choose appropriate materials to provide sufficient pavement skid resistance, which is the most straightforward way to generate enough anti-polishing ability.